

CAR-mediated targeting of NK cells overcomes tumor immune escape caused by ICAM-1 downregulation

Jiri Eitler ^{1,2,3}, Wiebke Rackwitz,^{1,2} Natalie Wotschel,^{1,2} Venugopal Gudipati,⁴ Nivedha Murali Shankar,^{1,2} Anastasia Sidorenkova,^{1,2} Johannes B Huppa ⁴, Paola Ortiz-Montero,^{1,2} Corinna Opitz,² Stephan R Künzel,^{1,2} Susanne Michen,⁵ Achim Temme,^{5,6} Liliana Rodrigues Loureiro,⁷ Anja Feldmann,^{3,7,8} Michael Bachmann,^{3,7,8} Laurent Boissel,⁹ Hans Klingemann,⁹ Winfried S Wels ^{10,11,12}, Torsten Tonn ^{1,2,3}

To cite: Eitler J, Rackwitz W, Wotschel N, *et al.* CAR-mediated targeting of NK cells overcomes tumor immune escape caused by ICAM-1 downregulation. *Journal for ImmunoTherapy of Cancer* 2024;**12**:e008155. doi:10.1136/jitc-2023-008155

► Additional supplemental material is published online only. To view, please visit the journal online (<http://dx.doi.org/10.1136/jitc-2023-008155>).

JE and WR contributed equally.
Accepted 24 December 2023



© Author(s) (or their employer(s)) 2024. Re-use permitted under CC BY-NC. No commercial re-use. See rights and permissions. Published by BMJ.

For numbered affiliations see end of article.

Correspondence to
Professor Torsten Tonn;
t.tonn@blutspende.de

Dr Jiri Eitler;
j.eitler@blutspende.de

ABSTRACT

Background The antitumor activity of natural killer (NK) cells can be enhanced by specific targeting with therapeutic antibodies that trigger antibody-dependent cell-mediated cytotoxicity (ADCC) or by genetic engineering to express chimeric antigen receptors (CARs). Despite antibody or CAR targeting, some tumors remain resistant towards NK cell attack. While the importance of ICAM-1/LFA-1 interaction for natural cytotoxicity of NK cells is known, its impact on ADCC induced by the ErbB2 (HER2)-specific antibody trastuzumab and ErbB2-CAR-mediated NK cell cytotoxicity against breast cancer cells has not been investigated.

Methods Here we used NK-92 cells expressing high-affinity Fc receptor FcγR11a in combination with trastuzumab or ErbB2-CAR engineered NK-92 cells (NK-92/5.28.z) as well as primary human NK cells combined with trastuzumab or modified with the ErbB2-CAR and tested cytotoxicity against cancer cells varying in ICAM-1 expression or alternatively blocked LFA-1 on NK cells. Furthermore, we specifically stimulated Fc receptor, CAR and/or LFA-1 to study their crosstalk at the immunological synapse and their contribution to degranulation and intracellular signaling in antibody-targeted or CAR-targeted NK cells.

Results Blockade of LFA-1 or absence of ICAM-1 significantly reduced cell killing and cytokine release during trastuzumab-mediated ADCC against ErbB2-positive breast cancer cells, but not so in CAR-targeted NK cells. Pretreatment with 5-aza-2'-deoxycytidine induced ICAM-1 upregulation and reversed NK cell resistance in ADCC. Trastuzumab alone did not sufficiently activate NK cells and required additional LFA-1 co-stimulation, while activation of the ErbB2-CAR in CAR-NK cells induced efficient degranulation independent of LFA-1. Total internal reflection fluorescence single molecule imaging revealed that CAR-NK cells formed an irregular immunological synapse with tumor cells that excluded ICAM-1, while trastuzumab formed typical peripheral supramolecular activation cluster (pSMAC) structures. Mechanistically, the absence of ICAM-1 did not affect cell–cell adhesion during ADCC, but rather resulted in decreased signaling via Pyk2 and ERK1/2, which was intrinsically provided by CAR-mediated targeting. Furthermore, while stimulation of the inhibitory NK cell checkpoint molecule NKG2A

WHAT IS ALREADY KNOWN ON THIS TOPIC

⇒ Redirecting natural killer (NK) cells by antibodies (antibody-dependent cell-mediated cytotoxicity (ADCC)) or chimeric antigen receptors (CARs) has been shown to be effective against a variety of otherwise NK-resistant cancer cells.

WHAT THIS STUDY ADDS

⇒ Here, we demonstrated that downregulation of the adhesion molecule ICAM-1 is a critical tumor escape mechanism from ErbB2-specific monoclonal antibodies trastuzumab-mediated NK cell cytotoxicity, whereas NK cells genetically engineered to express an ErbB2-specific CAR can overcome this resistance by bypassing LFA-1 signaling. This observation is new for CAR-NK cells and seems to distinguish them from what is known for CAR-T cells, which apparently still rely on additional LFA-1/ICAM-1 signals.

HOW THIS STUDY MIGHT AFFECT RESEARCH, PRACTICE OR POLICY

⇒ These data suggest that ADCC in patients with ICAM-1 low/negative cancers may be less effective. Strategies to upregulate ICAM-1 expression in tumors and/or the use of CAR engineered NK cells may represent a suitable strategy to leverage the NK cell response in patients with cancer.

markedly reduced FcγR11a/LFA-1-mediated degranulation, retargeting by CAR was only marginally affected.

Conclusions Downregulation of ICAM-1 on breast cancer cells is a critical escape mechanism from trastuzumab-triggered ADCC. In contrast, CAR-NK cells are able to overcome cancer cell resistance caused by ICAM-1 reduction, highlighting the potential of CAR-NK cells in cancer immunotherapy.

BACKGROUND

Natural killer (NK) cells are highly effective in recognizing and eliminating virus-infected

or malignant cells. Because of their unique anticancer properties, NK cells are very attractive for the development of cell-based cancer immunotherapies.¹ For adoptive transfer, NK cells can be isolated from peripheral and cord blood of healthy donors, or differentiated from hematopoietic or induced pluripotent stem cells.^{2–4} Alternatively, phenotypically stable NK cell lines are being considered as promising therapeutics, and in the case of NK-92 cells, have entered clinical trials.^{5,6}

Natural cytotoxicity of NK cells is tightly orchestrated by cumulative signals from germline-encoded activating and inhibitory receptors. These signaling networks are naturally programmed to trigger cytotoxicity on encountering diseased cells while maintaining tolerance to healthy tissues.⁷ Although NK cells are in principle able to eliminate many types of transformed cells, certain tumors still evade NK cell-mediated killing, limiting the efficacy of NK cell-based immunotherapies. Different resistance mechanisms that enable cancer cells to escape from NK cell cytotoxicity have been described,⁸ including downregulation of activating and upregulation of inhibitory ligands on tumor cells, which results in insufficient triggering of cytotoxic signals.^{9–11}

To enhance activating signals, monoclonal antibodies (mAbs) such as ErbB2 (HER2)-specific trastuzumab are infused into a patient, where they can opsonize tumor cells and bind via their Fc region to Fcγ receptor IIIa (FcγRIIIa, CD16) on endogenous NK cells, thereby triggering antibody-dependent cell-mediated cytotoxicity (ADCC). Alternatively, mAbs can be combined with adoptive transfer of donor-derived primary NK cells or clinically applicable NK cell lines such as high-affinity FcγRIIIa-modified NK-92 cells (haNK).¹² Treatment regimens based on trastuzumab are the clinical standard of care for ErbB2-positive breast cancer. Nevertheless, not all patients benefit from this therapy, with treatment resistance developing despite continued presence of the target antigen.¹³ Although ADCC is considered an important effector mechanism of trastuzumab in breast cancer,¹⁴ parameters predicting ADCC efficacy are not well established.

In recent years, NK cells genetically engineered with chimeric antigen receptors (CARs) have been introduced as a novel approach to target NK cells specifically to tumors and enhance their antitumor activity.¹⁵ An initial clinical study demonstrated encouraging efficacy of CD19-specific CAR-NK cells in hematologic malignancies comparable to that reported for CD19-CAR T cells, but without observing major side effects typical for CAR-T cell therapies.² In contrast to hematological malignancies, in clinical trials in solid tumor indications efficacy of CAR-T cells is still limited.¹⁶ Also CAR-NK cells are being investigated in early phase clinical trials for the treatment of solid tumors. In a current phase I trial (CAR2BRAIN; NCT03383978) patients with recurrent ErbB2-positive glioblastoma are treated with ErbB2-targeted CAR-NK-92 cells (NK-92/5.28.z). Data from the dose-escalation part of this study so far demonstrated safety and feasibility of

intracranial injections of these cells, with evaluation of NK-92/5.28.z in combination with an anti-programmed cell death protein 1 (PD-1) immune checkpoint inhibitor ongoing.¹⁷ Similar to tumor-specific targeting of NK cells with antibodies and induction of ADCC, a better understanding of the signals required for CAR-NK cells to efficiently eliminate cancer cells of solid tumor origins is critical for the success of these cell-based advanced therapy medicinal products.

We previously showed that tumor-specific targeting of NK cells mediated either by combination with an antibody or expression of a CAR can provide the necessary signals to direct cytotoxic granules to the immunological synapse and enable secretion of the lytic enzymes toward otherwise NK-resistant cancer cells.¹⁸ However, it is not clear at present whether CAR-mediated or FcγRIIIa-mediated signals alone are sufficient to overcome NK-resistance, or whether synergistic mechanisms are required for efficient NK cell cytotoxicity. For example, adhesion molecules are known to play an important role for NK cell potency. Thereby, LFA-1 is essential for efficient natural cytotoxicity of NK cells, as it initiates the assembly of the immunological synapse and mediates firm adhesion to the target, which contributes to NK cell activation.¹⁹ Signaling through the cell adhesion molecule LFA-1 after binding to its natural ligand ICAM-1 on tumor cells is a prerequisite for targeted convergence of lytic granules toward the immunological synapse, allowing for maximum on-target efficiency with minimal collateral damage.^{20,21} Conversely, ICAM-1 can be downregulated or shed by tumor cells, leading to insufficient LFA-1 activation or decreased cell adhesion due to receptor blockade.^{22–24} While in hematological malignancies downregulation of ICAM-1 on acute myeloid leukemia (AML) cells led to escape from natural NK cell cytotoxicity,²⁵ the role of ICAM-1 in solid tumors has not yet been investigated with respect to NK cell activation. Nevertheless, a dysregulated interferon (IFN)-γ pathway in CAR-T cells was recently shown to result in low ICAM-1 expression in solid tumors, leading to escape from CAR-T cell-mediated killing.²⁶

While this suggests a critical role of cell adhesion molecules for CAR-T cell-based therapies, the relevance of ICAM-1 expression in NK cells for ADCC and CAR-mediated killing is presently unknown. In particular, it is unclear whether downregulation or cleavage of ICAM-1 on breast cancer cells can lead to escape from trastuzumab-mediated ADCC or CAR-induced cytotoxicity of NK cells. However, considering the limited efficacy of trastuzumab in some patients with breast cancer and the need to improve treatment approaches with CAR-engineered effector cells for solid tumor indications, a better understanding of such tumor escape mechanisms is of high clinical relevance.

Here, we investigated the role of ICAM-1/LFA-1 interaction and LFA-1-dependent stimulation in trastuzumab-induced ADCC of FcγRIIIa-expressing NK cells or CAR-mediated cytotoxicity of ErbB2-CAR-NK cells against ErbB2-positive breast cancer cells.

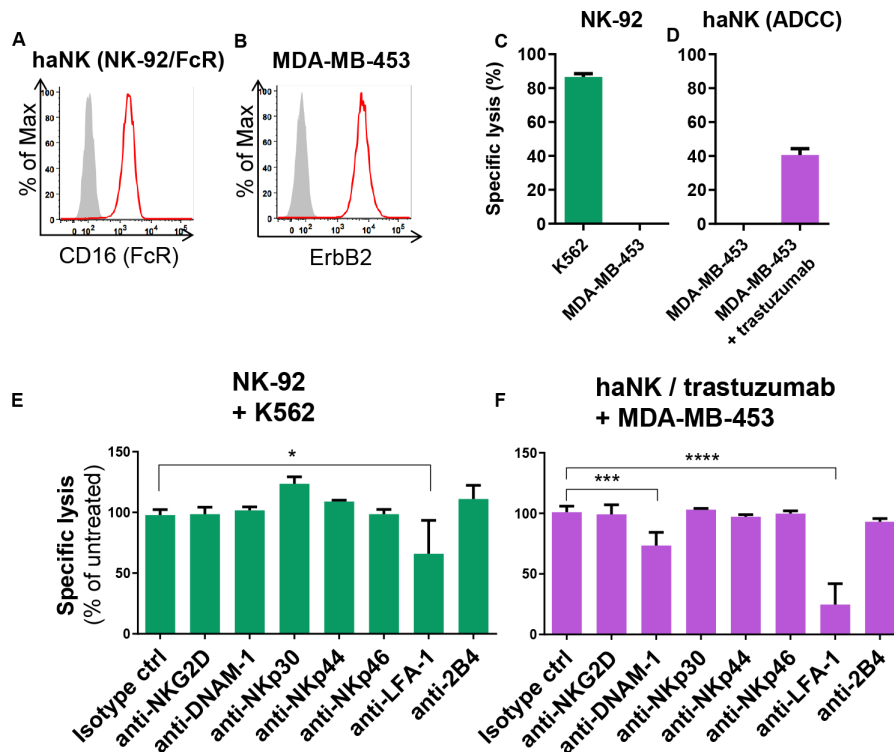


Figure 1 Blockade of LFA-1 alleviates natural cytotoxicity and ADCC of NK cells. (A, B) Histograms confirm FcγRIIIa (CD16) expression on haNK cells (A) and ErbB2 expression on MDA-MB-453 breast cancer cells (B). Filled gray areas indicate isotype controls. Representative data from at least three independent experiments are shown. (C, D) NK-92 (C) or haNK (D) cells were co-cultured with K562 or MDA-MB-453 cells at an effector to target ratio of 10:1 for 2 hours, and specific cytotoxicity was measured using a Europium-based cytotoxicity assay. Trastuzumab was added where indicated at a concentration of 2 μg/mL. Mean values from three independent experiments ± SEM are shown. (E, F) The indicated receptors on NK-92 (E) or haNK (F) cells were blocked with specific antibodies (20 μg/mL) for 60 min, followed by 2 hours co-culture with K562 or MDA-MB-453 cells. Isotype control IgG1 is shown (IgG2b was comparable). Trastuzumab (2 μg/mL) was added as indicated. Specific cytotoxicity was measured using a Europium-based cytotoxicity assay and is depicted as the percentage of cytotoxicity in the absence of blocking antibodies. Data were pooled from at least three independent experiments. Mean values ± SEM are shown. ADCC, antibody-dependent cell-mediated cytotoxicity; haNK, high-affinity FcγRIIIa-modified NK-92 cells; NK, natural killer.

MATERIALS AND METHODS

Materials and methods are available in the online supplemental material.

RESULTS

Co-stimulatory signals are required for effective ADCC

Previously, we demonstrated that ErbB2 (HER2)-specific antibody trastuzumab, when bound to FcγRIIIa (CD16) of NK cells, triggers their activation, granule polarization and subsequent cytotoxicity against ErbB2-expressing tumor cells.¹⁸ Nevertheless, it remained unclear to what extent additional signaling pathways contribute to efficient trastuzumab-mediated ADCC. Hence, we tested whether other NK cell activating or co-stimulatory receptors synergize with FcγRIIIa activation. We used haNK cells, an NK-92 cell line expressing high-affinity FcγRIIIa¹² (figure 1A) in combination with the therapeutic antibody trastuzumab as a model. NK-92 cells are phenotypically and functionally similar to activated primary NK cells, except that NK-92 cells do not express KIRs that interact with HLA molecules.²⁷

Therefore, the NK-92 model allows the study of ADCC in the absence of HLA-mediated NK inhibition. As target cells, we employed the ErbB2-expressing breast cancer cell line MDA-MB-453 (figure 1B). Consistent with previous studies,^{18,28} NK-92 cells were highly cytotoxic to NK-sensitive K562 cells, whereas MDA-MB-453 cells proved resistant to natural NK-92 cytotoxicity (figure 1C). Likewise, in agreement with previous study,¹² in the absence of trastuzumab MDA-MB-453 cells were also resistant to haNK cells, but readily killed by haNK cells via ADCC in the presence of the ErbB2-specific IgG1 antibody (figure 1D). To test potential contribution of signals from other activating receptors or adhesion molecules to trastuzumab-mediated ADCC, we co-cultured MDA-MB-453 cells with haNK cells and trastuzumab in the presence of antibodies that block the NK cell activating receptors NKG2D, NKp30, NKp44, NKp46 or DNAM-1, co-stimulatory 2B4, or the adhesion molecule LFA-1. We found that blockade of LFA-1, and to a lesser extent DNAM-1, reduced trastuzumab-mediated ADCC (figure 1F). Natural cytotoxicity of NK-92 against K562 cells was

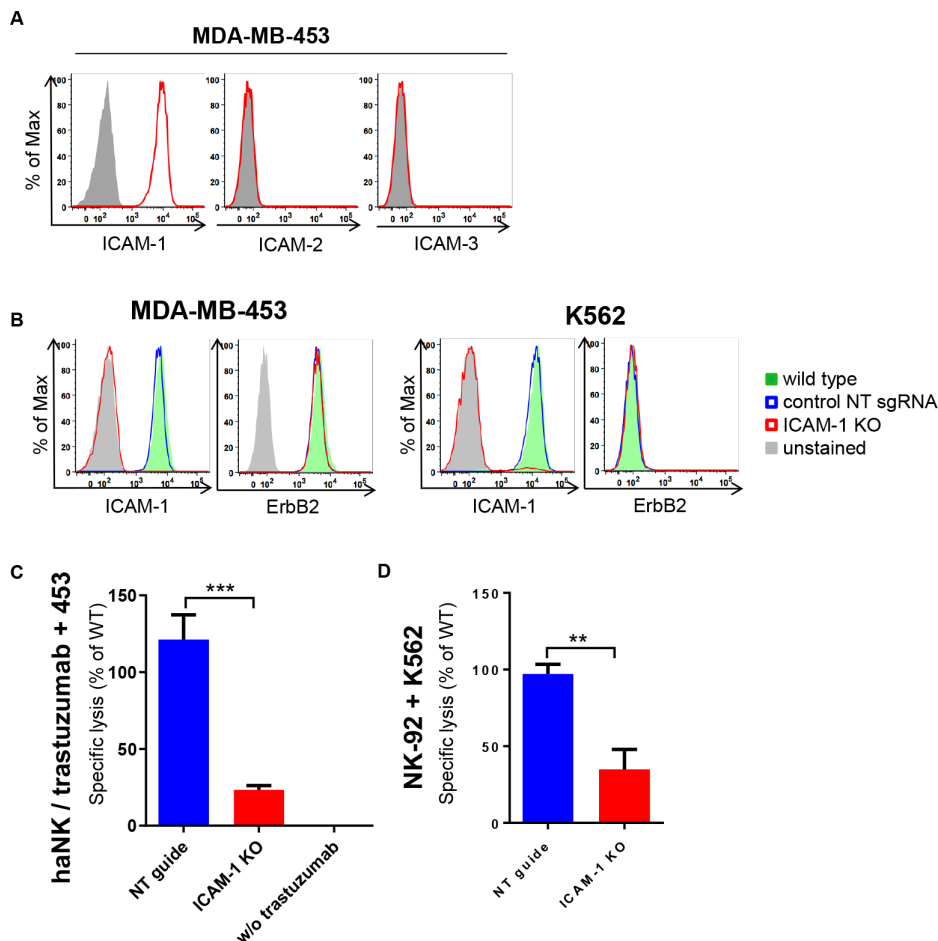


Figure 2 Downregulation of ICAM-1 results in escape from trastuzumab-mediated ADCC. (A) Flow cytometric analysis of ICAM-1, ICAM-2, and ICAM-3 expression on MDA-MB-453 cells. Filled gray areas indicate isotype controls. (B) ICAM-1 and ErbB2 expression on K562 and MDA-MB-453 ICAM-1 knock-out (KO) cells, and non-targeting sgRNA transduced (NT) or parental wild type (WT) control cells. Representative data from at least three independent experiments are shown. (C, D) haNK cells combined with trastuzumab (C) or NK-92 (D) cells were co-cultured for 2 hours with MDA-MB-453 or K562 ICAM-1 KO or NT and parental WT control cells at an effector to target ratio of 10:1 as indicated. Specific cytotoxicity was measured using a Europium-based cytotoxicity assay. Values for ICAM-1 KO and NT control cells are plotted relative to those obtained with parental WT MDA-MB-453 or K562 cells. To confirm trastuzumab-mediated ADCC against MDA-MB-453 cells, control samples without trastuzumab were included. Data were pooled from at least three independent experiments. Mean values \pm SEM are shown. ADCC, antibody-dependent cell-mediated cytotoxicity; haNK, high-affinity Fc γ R1IIIA-modified natural killer-92 cells.

only affected by blockade of LFA-1 (figure 1E). These data indicate that signaling via LFA-1 and DNAM-1 is required for effective trastuzumab-triggered cytotoxicity, whereas natural cytotoxicity of the NK cells depends in part on LFA-1.

ICAM-1 downregulation facilitates escape from trastuzumab-mediated NK cell killing

Next, we investigated which ligands on MDA-MB-453 cells stimulate LFA-1 on NK cells. Flow cytometric analysis of the most common LFA-1 ligands ICAM-1, ICAM-2 and ICAM-3 showed that only ICAM-1 is expressed on the surface of MDA-MB-453 cells (figure 2A). Thus, we hypothesized that decreased ICAM-1 expression may affect trastuzumab-mediated killing. We used CRISPR/Cas9 to generate ICAM-1 knockout (ICAM-1 KO) MDA-MB-453 and K562 cells, which in the case of MDA-MB-453 still displayed high ErbB2 expression (figure 2B). ICAM-1

and ErbB2 levels in cells edited with control non-targeting (NT) sgRNA did not differ from those of the parental wild type (WT) cells. Subsequently, we tested NK cytotoxicity toward these different target cells. Thereby, haNK cells in combination with trastuzumab showed high cell killing activity against MDA-MB-453 WT and MDA-MB-453 NT control cells, while cytotoxicity toward MDA-MB-453 ICAM-1 KO cells was markedly reduced (figure 2C). Similarly, natural cytotoxicity of NK-92 cells against K562 ICAM-1 KO cells was decreased when compared with K562 NT control cells (figure 2D). Accordingly, ICAM-1 downregulation can contribute to escape from natural and trastuzumab-mediated killing by NK cells.

ErbB2-specific CAR-NK cells overcome immune escape caused by ICAM-1 downregulation

Similar to ADCC, CAR-expression in NK cells can trigger targeted cytotoxicity against otherwise NK-resistant cancer

cells, but does not depend on antibody-mediated Fc γ RIIIa activation. To determine whether ICAM-1 downregulation in tumor cells can also affect CAR-mediated killing, we employed the clinically applied ErbB2-specific CAR NK-92 cell line NK-92/5.28.z (figure 3A).^{17,28} In contrast to parental NK-92, NK-92/5.28.z cells are highly cytotoxic against MDA-MB-453 cells (figure 3B). Interestingly, we did not observe a significant reduction in CAR-mediated cytotoxicity toward MDA-MB-453 ICAM-1 KO compared with NT control cells. Similarly, blockade of LFA-1 did not affect CAR-mediated cytotoxicity (figure 3C). To investigate the contribution of ICAM-1 to CAR-independent natural cytotoxicity of NK-92/5.28.z cells, we co-cultured them with ErbB2-negative but NK-sensitive K562 cells. As expected, NK-92/5.28.z killed K562 NT control cells, while cytotoxicity toward K562 ICAM-1 KO was markedly reduced, comparable to parental NK-92 cells. Similar results were obtained when LFA-1 on NK-92/5.28.z cells was blocked (figure 3D). These data indicate that in contrast to natural cytotoxicity, CAR-mediated killing by NK-92/5.28.z cells is ICAM-1 independent. To analyze whether this finding can be generalized, we also tested the ICAM-1-positive and ErbB2-positive breast and pancreatic cancer cell lines MCF-7 and BxPc3 (figure 3E). Similar to the results obtained with MDA-MB-453 breast cancer cells, in both cell lines blockade of LFA-1 reduced trastuzumab-mediated ADCC of haNK cells, while CAR-mediated cytotoxicity by NK-92/5.28.z cells remained unaffected (figure 3F). To test whether this is also the case with primary NK cells, we transduced primary human peripheral blood NK (pNK) cells with an ErbB2-specific CAR construct.²⁸ pNK cells had a purity of 95 \pm 1%, and CAR expression was detected in 35 \pm 1% of the transduced cells (online supplemental figure S1 A and B). ADCC was tested by combining unmodified pNK cells with trastuzumab. As shown in figure 3G, both, pNK cells in combination with trastuzumab and CAR-modified pNK cells effectively killed MDA-MB-453 WT cells, while only CAR pNK cells were able to effectively eliminate MDA-MB-453 ICAM-1 KO cells, which were resistant to trastuzumab-mediated ADCC by pNK cells. Accordingly, CAR-mediated targeting of established NK-92 and primary NK cells can both overcome immune escape caused by ICAM-1 downregulation.

CAR-NK cells retain ICAM-1 independent cytotoxicity and cytokine production during long-term interaction with cancer cells

To challenge CAR-NK cells with ICAM-1 negative targets for a longer time period, we mixed CytoLightRed-labeled MDA-MB-453 ICAM-1 KO cells with NK-92/5.28.z cells, or haNK cells combined with trastuzumab at an effector to target ratio of 1:1, and co-cultured them for 50 hours (figure 4A). The co-cultures were monitored every 6 hours using the InCuCyte live-cell imaging system, and cytotoxicity was quantified based on the proportion of viability dye-positive cancer cells (figure 4B and C). In agreement with our data from short-term assays, both, the absence of ICAM-1 on cancer cells and LFA-1 blockade on NK cells

resulted in a marked reduction of trastuzumab-induced ADCC of haNK cells against MDA-MB-453 target cells. Again, CAR-engineered NK-92/5.28.z cells were unaffected by the loss of ICAM-1 on tumor cells and able to kill MDA-MB-453 ICAM-1 KO cells as efficiently as the control targets. Likewise, LFA-1 blockade on NK-92/5.28.z cells did not affect CAR-mediated cytotoxicity. LFA-1 expression on NK-92, haNK and NK-92/5.28.z cells was comparable (figure 4D), ruling out potential differences in initial LFA-1 levels. In addition to direct target cell killing, the production of cytokines like IFN- γ , tumor necrosis factor alpha (TNF- α) or chemokines such as macrophage inflammatory protein 1-alpha (MIP-1 α) is important for the antitumor activity of NK cells. MIP-1 α has also been reported to be induced by LFA-1 stimulation.²⁹ Hence, we tested whether cytokine production accompanying ADCC or CAR-mediated NK cell cytotoxicity is affected in the absence of ICAM-1/LFA-1 interaction. We co-cultured haNK cells in combination with trastuzumab or NK-92/5.28.z cells with MDA-MB-453 ICAM-1 KO or parental WT cells after blockade of LFA-1 on the NK cells, and measured cytokine release in the supernatants after 6 hours of co-culture. As expected, exposure to MDA-MB-453 WT cells resulted in the production of IFN- γ , TNF- α and MIP-1 α by haNK cells combined with trastuzumab and NK-92/5.28.z cells (figure 4E and F). In contrast, co-culture with MDA-MB-453 ICAM-1 KO cells did not induce any measurable TNF- α and significantly reduced the amounts of IFN- γ and MIP-1 α produced by haNK cells combined with trastuzumab, while cytokine production by NK-92/5.28.z cells was unaffected by the lack of ICAM-1. Consistent with these results, LFA-1 blockade only reduced cytokine production by haNK cells combined with trastuzumab, but not by CAR-engineered NK-92/5.28.z cells.

Pharmacological intervention improves trastuzumab-mediated ADCC against ICAM-1^{low} cancer cells

The data obtained in our models suggest that trastuzumab therapy in patients with cancers expressing low levels of ICAM-1 may result in low efficacy or treatment failure. To investigate whether pharmacological intervention to upregulate ICAM-1 can improve trastuzumab-mediated NK cell cytotoxicity, we applied the clinically used DNA methyltransferase inhibitor 5-aza-2'-deoxycytidine (5AZA), previously shown to increase ICAM-1 expression in cancer cells.²⁵ As a model, we employed HEK293 cells which are ICAM-1 low/negative but express moderate levels of ErbB2. Indeed, treatment with 5AZA increased ICAM-1 expression in HEK293 cells, while ErbB2 expression remained unchanged (figure 5A). Consistent with this, 5AZA treatment increased trastuzumab-mediated ADCC of haNK cells 1.8-fold compared with untreated control cells, while CAR-mediated cytotoxicity of NK-92/5.28.z against 5AZA-treated cells was comparable to that against untreated control targets (figure 5B and C). Also cytokines like TNF- α and IFN- γ have been reported to upregulate ICAM-1 in cancer cells.^{26,30}

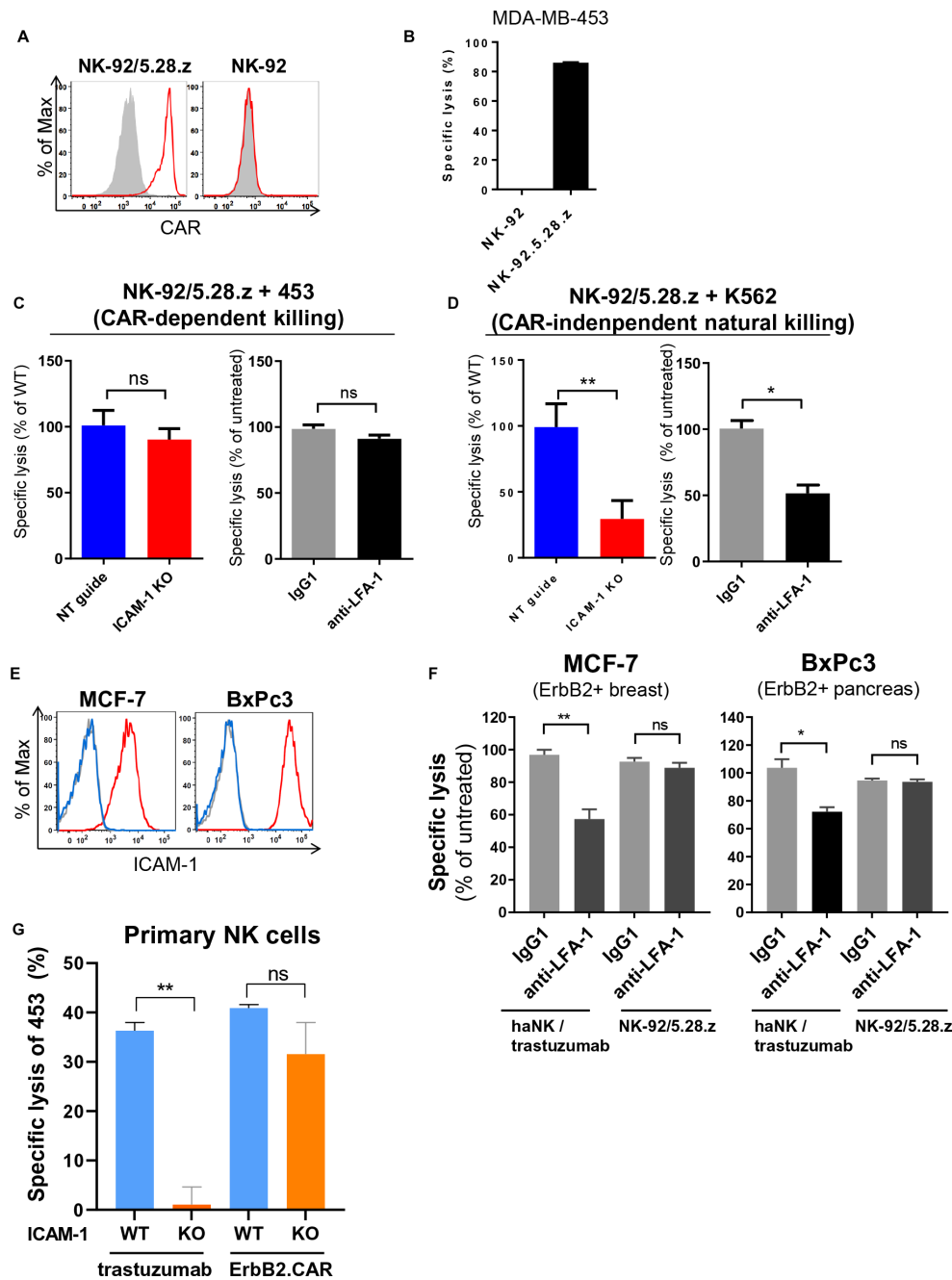


Figure 3 CAR-mediated targeting overcomes immune escape caused by ICAM-1 downregulation. (A) CAR expression on NK-92/5.28.z cells (left) was detected by flow cytometry using human recombinant ErbB2-Fc protein followed by anti-Fc secondary antibody. Parental NK-92 cells (right) were included for comparison. Filled gray areas indicate negative controls only stained with secondary antibody. Representative data from at least three independent experiments are shown. (B) Specific cytotoxicity of NK-92/5.28.z against MDA-MB-453 cells was measured using a Europium-based assay after 2 hours of co-culture at an effector to target ratio of 10:1. (C) Specific CAR-mediated cytotoxicity of NK-92/5.28.z against MDA-MB-453 ICAM-1 KO, NT and WT cells (left) and against WT cells following incubation of NK-92/5.28.z cells with LFA-1 blocking antibody or control IgG for 60 min prior to co-culture (right). (D) Natural cytotoxicity of NK-92/5.28.z against K562 ICAM-1 KO, NT and WT cells (left) and against WT cells following incubation of NK-92/5.28.z cells with LFA-1 blocking antibody or control IgG for 60 min prior to co-culture (right). (E) Flow cytometric analysis of ICAM-1 expression on MCF-7 breast and BxPc3 pancreatic cancer cells. Blue lines indicate isotype controls and gray lines indicate unstained controls. (F) Specific cytotoxicity of haNK cells in combination with trastuzumab or CAR-engineered NK-92/5.28.z cells against MCF-7 and BxPc3 cells. NK cells were pretreated with LFA-1 blocking antibody or control IgG as indicated. Cytotoxicity data were pooled from at least three independent experiments. Mean values \pm SEM are shown. (G) Primary NK cells modified with an ErbB2-specific CAR or combined with trastuzumab were co-cultured with MDA-MB-453 ICAM-1 KO or WT cells for 2 hours and specific cytotoxicity was measured using a Europium-based assay. Representative data from three independent experiments using three different donors are depicted. Mean values \pm SEM are shown. CAR, chimeric antigen receptor; haNK, high-affinity Fc γ R1IIa-modified NK-92 cells; KO, knockout; NK, natural killer; NT, non-targeting; WT, wild type.

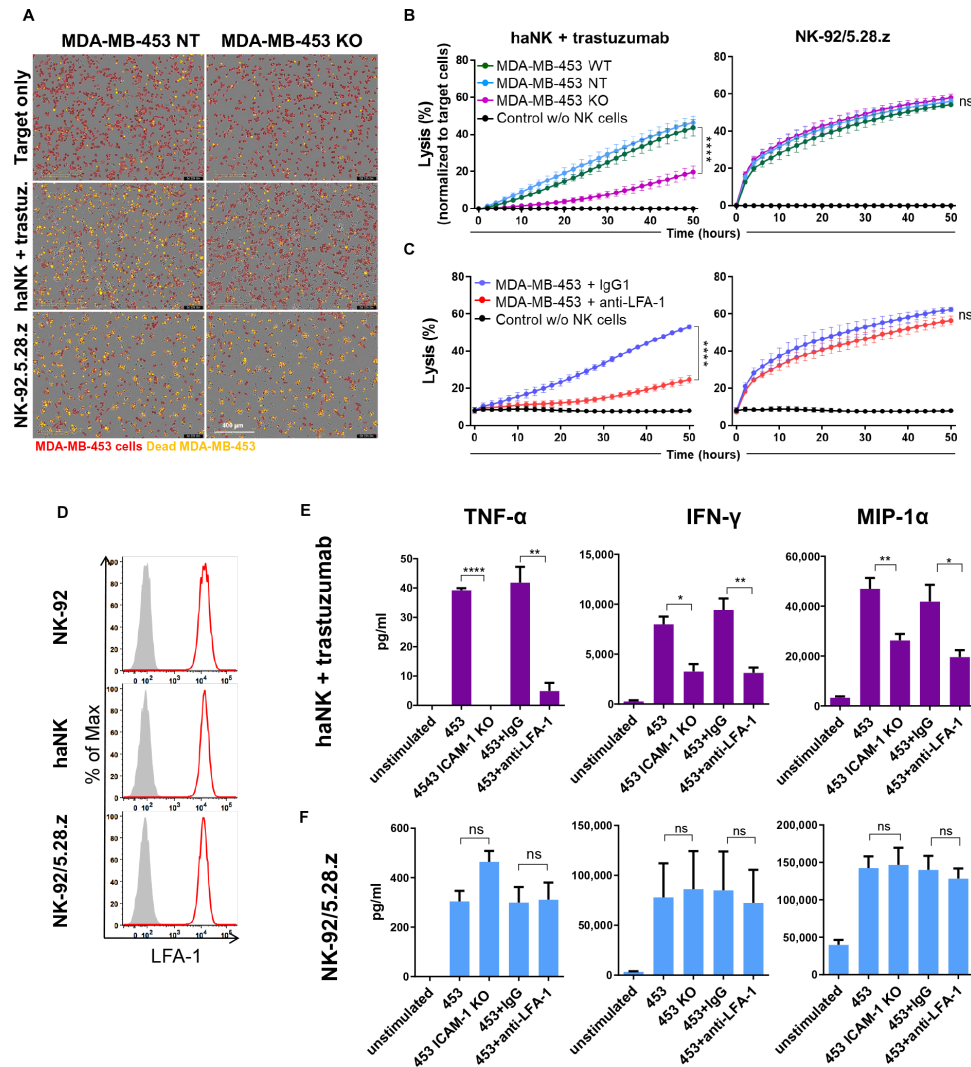


Figure 4 CAR-NK cells retain ICAM-1-independent activity and cytokine production in long-term killing assays. (A–C) MDA-MB-453 ICAM-1 KO, NT and WT control cells were labeled with CytoLightRed and allowed to adhere to 96-well plates. NK-92/5.28.z CAR-NK cells or haNK cells in combination with trastuzumab were added at an E:T ratio of 1:1 in medium supplemented with CytoToxGreen viability dye, and cytotoxicity over time was analyzed using the IncuCyte live-cell imaging system. Where indicated, NK cells were treated with LFA-1 blocking antibody or control IgG1 prior to co-culture. (A) Microscopic images showing the co-cultures after 50 hours, with MDA-MB-453 cells labeled in red. Overlapping red and green signals (yellow) indicate dead MDA-MB-453 cells. (B, C) Graphs depicting cytotoxicity at the indicated time points calculated as the percentage of dead (double-positive) cancer cells out of total (red) cancer cells. Data were pooled from at least three independent experiments. Mean values \pm SEM are shown. Statistical analysis was performed using two-way analysis of variance. (D) Flow cytometric analysis of LFA-1 expression on NK-92, haNK and NK-92/5.28.z cells. Filled gray areas indicate isotype controls. Representative data out of at least three independent experiments are shown. (E, F) haNK cells combined with trastuzumab (E) or NK-92/5.28.z cells (F) were co-cultured with MDA-MB-453 ICAM-1 KO or WT cells at an E:T ratio of 1:1 for 6 hours in duplicates. Where indicated, NK cells were treated with LFA-1 blocking antibody or control IgG prior to co-culture. Supernatants from duplicate samples were pooled, and cytokine concentrations were measured using the ProcartaPlex Luminex system. Mean values \pm SEM calculated from three independent experiments are shown. CAR, chimeric antigen receptor; E:T, effector to target; haNK, high-affinity Fc γ RIIIa-modified NK-92 cells; IFN, interferon; KO, knockout; NK, natural killer; NT, non-targeting; MIP-1 α , macrophage inflammatory protein 1-alpha; TNF- α , tumor necrosis factor alpha; WT, wild type.

As shown above, high amounts of these cytokines are secreted by activated NK cells (see [figure 4E and F](#)). When we treated HEK293 cells with recombinant TNF- α , we observed upregulation of ICAM-1, but no influence of the cytokine on ErbB2 expression ([figure 5D](#)). Consequently, HEK293 treated with TNF- α were more sensitive to trastuzumab-mediated ADCC by haNK cells ([figure 5E and F](#)). In contrast, as in the case after 5AZA treatment,

CAR-mediated cytotoxicity of NK-92/5.28.z remained unchanged. Next, we tested whether 5AZA and TNF- α can further enhance trastuzumab-mediated NK cell cytotoxicity against cancer cells with high levels of ICAM-1. In ICAM-1 high MDA-MB-453 cells, we observed further upregulation of ICAM-1 after treatment with TNF- α , but not after treatment with 5AZA (online supplemental [figure S3A](#)). As expected, in MDA-MB-453 ICAM-1 KO,

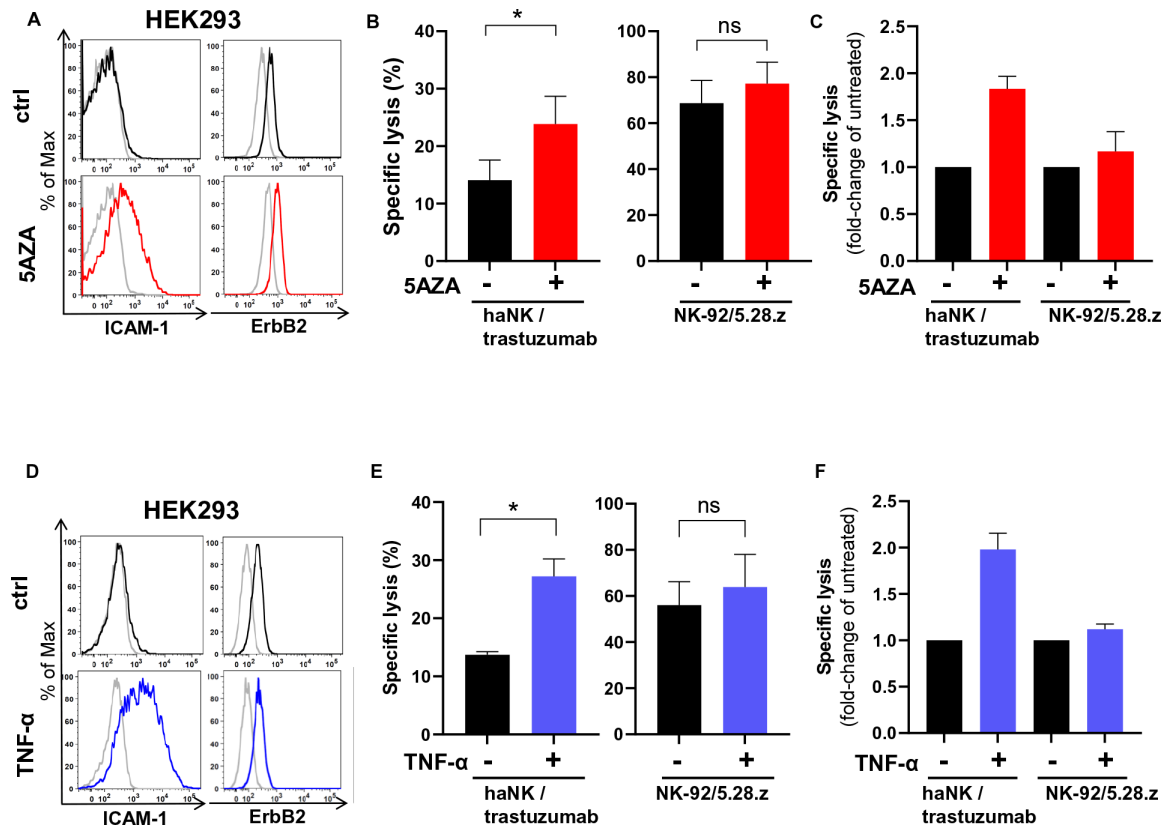


Figure 5 Treatment with 5-aza-2'-deoxycytidine or TNF- α upregulates ICAM-1 expression and improves trastuzumab-mediated NK cell cytotoxicity. (A, D) HEK293 cells were treated with 1 μ M 5-aza-2'-deoxycytidine (5AZA) for 72 hours (A) or with 100 ng/mL TNF- α for 48 hours (D). Expression of ICAM-1 and ErbB2 was analyzed by flow cytometry. Representative histograms are shown. (B, E) haNK cells combined with trastuzumab, or CAR-engineered NK-92/5.28.z cells were incubated for 2 hours with HEK293 cells pretreated with 5AZA (B) or TNF- α (E). Specific cytotoxicity was measured using a Europium-based cytotoxicity assay. (C, F) Specific lysis is depicted as fold-change in comparison to cytotoxicity of the NK cells against HEK293 control cells without 5AZA or TNF- α pretreatment. Data were pooled from three independent experiments. Mean values \pm SEM are shown. CAR, chimeric antigen receptors; haNK, high-affinity Fc γ R1IIa-modified NK-92 cells; NK, natural killer; TNF- α , tumor necrosis factor alpha.

treatment with 5AZA or TNF- α did not increase ICAM-1 expression (online supplemental figure S3C). In WT MDA-MB-453 cells, 5AZA did not increase trastuzumab-mediated NK cell cytotoxicity, whereas TNF- α moderately increased haNK/trastuzumab cytotoxicity (although not statistically significant), which correlated with increased ICAM-1 expression levels (online supplemental figure S3B). As expected, when ICAM-1 KO MDA-MB-453 cancer cells were subjected to 5AZA or TNF- α treatment, the cytotoxicity was not improved (online supplemental figure S3D), indicating that 5AZA and TNF- α confer sensitivity to NK-mediated killing exclusively by upregulating ICAM-1 in ICAM-1-negative/low cancer cells. Taken together, these data suggest that treatment with 5AZA may enhance the efficacy of trastuzumab in patients with cancer with tumors with low ICAM-1 expression. In addition, secretion of TNF- α by activated NK cells may further upregulate ICAM-1 expression on cancer cells, thereby functioning as a maintenance or amplification loop.

CAR and LFA-1 do not interact at the immunological synapse of NK cells

Close contact between cancer and NK cells takes place at the immunological synapse, where directed cytotoxicity is orchestrated by activating and inhibitory receptors and ligands. To narrow down which molecules are minimally required for trastuzumab-mediated ADCC and CAR-mediated cytotoxicity, we immobilized single activating ligands or their combinations on a microtiter plate and measured the degranulation marker CD107a as a readout for NK cell activation. In the case of haNK cells, immobilized trastuzumab alone did not induce any degranulation events, and immobilized LFA-1-specific antibody only induced a low level of degranulation. In contrast, in combination trastuzumab and anti-LFA-1 induced strong degranulation (figure 6A and B). Conversely, at moderate and high concentrations, immobilized recombinant ErbB2 protein alone already induced strong degranulation in CAR-engineered NK-92/5.28.z cells, which was not enhanced any further by additional immobilized anti-LFA-1. Only when immobilized ErbB2 protein became

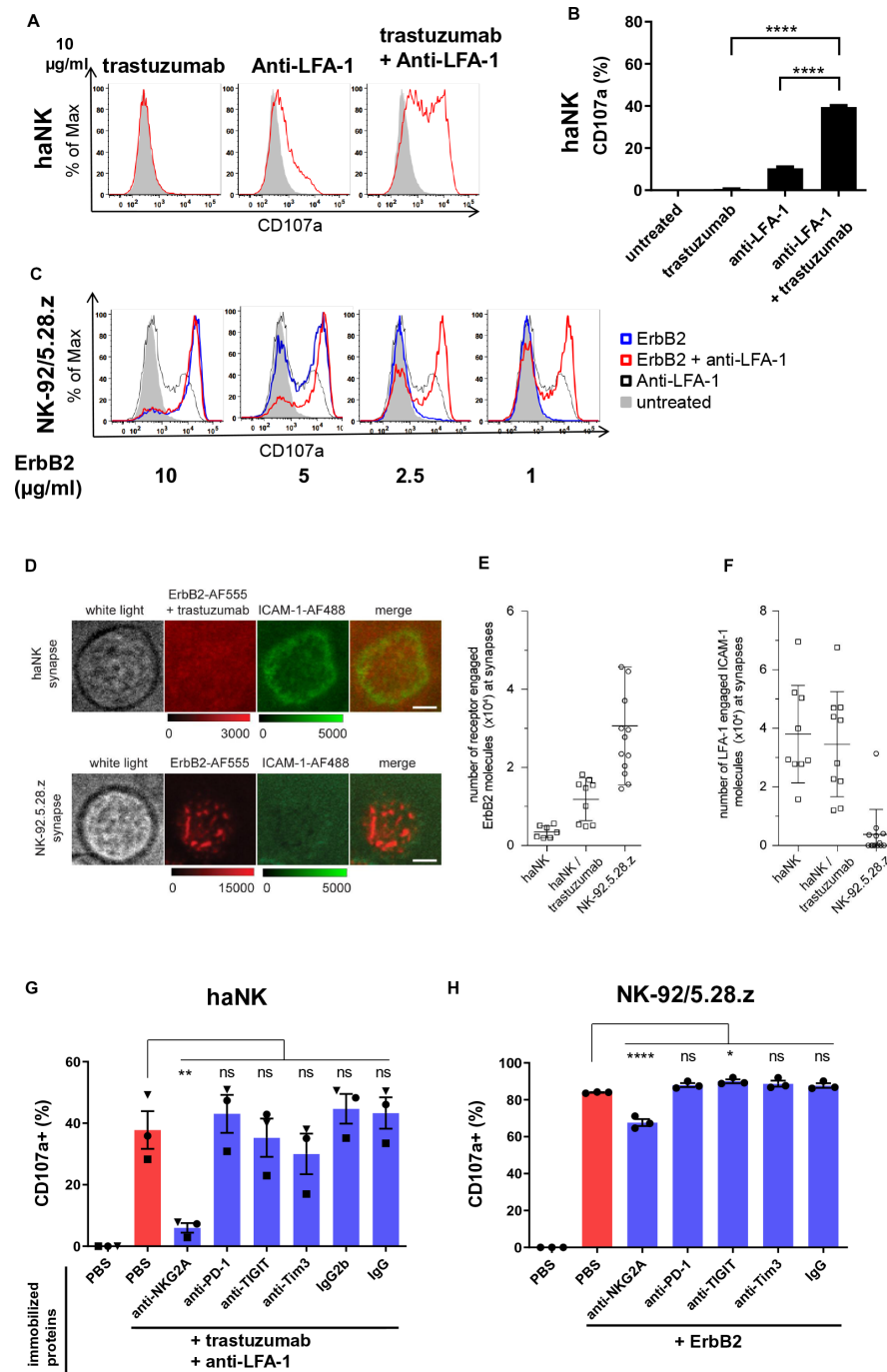


Figure 6 Chimeric antigen receptor-NK cells form an irregular immunological synapse, which is LFA-1 independent. (A) haNK cells were incubated with indicated plate-bound antibodies in the presence of labeled anti-CD107a antibody for 2 hours, followed by flow cytometric analysis of CD107a as a degranulation marker. Untreated NK cells are depicted in gray. (B) Quantification of CD107a expression. (C) NK-92/5.28.z cells were incubated with plate-bound ErbB2 protein in the presence of labeled anti-CD107a antibody for 2 hours, followed by flow cytometric analysis of CD107a. Representative data from three independent experiments are shown. (D) Total internal reflection fluorescence (TIRF) microscopy images displaying synaptic recruitment of fluorescently labeled ErbB2-AF555 and ICAM-1-AF488 molecules at the synapses of haNK cells in the presence of trastuzumab and NK-92.5.28.z cells. Scale bars: 5 μm . (E, F) Quantification of ErbB2-AF555 (E) and ICAM-1-AF488 (F) molecules recruited at the synapses of haNK and NK-92.5.28.z cells. Each data point represents the number of molecules recruited at the synapse of one cell. Mean values are indicated. Error bars represent \pm SD. (G, H) haNK cells were incubated with plate-bound trastuzumab and anti-LFA-1 (G) and NK-92/5.28.z with plate-bound ErbB2 protein (H) in each case combined with plate-bound antibodies targeting the indicated inhibitory receptors or immune checkpoint molecules, or respective isotype controls. Degranulation was measured by flow cytometric analysis of CD107a expression. Data were pooled from three independent experiments. Mean values \pm SEM are shown. haNK, high-affinity Fc γ RIIIa-modified NK-92 cells; NK, natural killer; PBS, phosphate-buffered saline; PD-1, programmed cell death protein 1; TIGIT, T cell immunoreceptor with Ig and ITIM domains; TIM-3, T-cell immunoglobulin and mucin-domain containing-3.

limiting at low concentrations, additional stimulation of LFA-1 synergized with CAR activation and increased the CD107a signal (figure 6C, online supplemental figure S2 A). These data suggest that the CAR does not require LFA-1 for degranulation if sufficient target antigen is present on the cancer cell.

To investigate indirect interaction of FcγRIIIa with ErbB2 via trastuzumab and direct interaction of the CAR with the antigen, and to follow recruitment of ICAM-1 by LFA-1 at the NK cell immunological synapse, we next employed single molecule resolution TIRF (total internal reflection fluorescence) microscopy. Thereby, precise quantitation of the number of antigens and co-stimulatory molecules at the interface of NK and target cell conjugates is challenging due to three-dimensional cellular movement and phototoxicity. To circumvent these limitations, we generated supported lipid layers (SLB) and loaded them with fluorescently labeled ErbB2 and ICAM-1 molecules as an artificial target cell surface. haNK cells combined with trastuzumab, and NK-92/5.28.z cells were seeded onto SLBs, and immunological synapses were imaged after 10 min in total internal reflection mode. We observed that both, haNK cells in the presence of trastuzumab, and NK-92/5.28.z cells displayed target antigen enrichment within their immunological synapses. At NK-92/5.28.z cell synapses, ErbB2 was recruited to discrete molecular clusters, whereas in haNK cells combined with trastuzumab the antigen was more homogeneously distributed (figure 6D). Next, we quantified the absolute numbers of ErbB2 and ICAM-1 molecules recruited to haNK and NK-92/5.28.z immunological synapses. We found that NK-92/5.28.z cells recruited approximately 2.6-times more ErbB2 molecules than haNK cells (figure 6E). In contrast, haNK cells recruited approximately 10-times more ICAM-1 than NK-92/5.28.z cells, and induced formation of distinct ICAM-1 rings (figure 6F). These data suggest that despite recruiting fewer ErbB2 molecules to their immunological synapse, haNK cells are more efficient in initiating LFA-1-mediated clustering of ICAM-1, while clustering of ICAM-1 at the NK-92/5.28.z immunological synapse appears to be dysregulated.

Subsequently, we investigated whether immune checkpoint molecules and inhibitory receptors can affect trastuzumab-mediated or CAR-mediated degranulation of NK cells. To enable maximum degranulation, haNK cells were activated with immobilized trastuzumab and anti-LFA-1, and NK-92/5.28.z cells with immobilized ErbB2. Additionally, we added immobilized antibodies specific for NKG2A, T cell immunoreceptor with Ig and ITIM domains (TIGIT), PD-1 and T-cell immunoglobulin and mucin-domain containing-3 (Tim-3) to initiate signal transduction from these receptors in the NK cells. We found that ADCC in haNK cells was inhibited by cross-linking of NKG2A, but not PD-1. Ligation of TIGIT or Tim-3 also reduced degranulation, but not to a statistically significant extent (figure 6G, online supplemental figure S2 B). Degranulation of NK-92/5.28.z cells in response to ErbB2 was moderately inhibited by NKG2A ligation, while

the other tested immune checkpoint molecules had no effect (figure 6H, online supplemental figure S2 B). We next tested whether this finding could be translated to cytotoxicity against HLA-E positive cancer cells. For this purpose, we blocked haNK/trastuzumab or NK-92/5.28.z cells with anti-NKG2A antibody and co-cultured them with ErbB2/HLA-E/ICAM-1 triple positive ovarian SKOV-3 cells (natural HLA-E expression) and glioblastoma HT18584-HLA-E cells, engineered to overexpress HLA-E (online supplemental figures S4A and S5A). Interestingly, we found no improvement in the cytotoxicity of either haNK/trastuzumab or NK-92/5.28.z in both short-term and long-term killing assays (online supplemental figures S4B,C and S5B). Taken together, these data demonstrate that engagement of LFA-1 at the immunological synapse of the NK cells is critical for trastuzumab-mediated degranulation, while CAR-mediated degranulation of NK cells is LFA-1 independent. NKG2A engagement can inhibit degranulation signals from FcγRIIIa/LFA-1 and partially also from CAR in an isolated artificial system. Analysis of cytotoxicity against tumor cells suggests that physiological inhibition of NKG2A by HLA-E may not be sufficient to confer resistance to ADCC or CAR-mediated NK cell killing in the tested cancer cells and that additional unknown inhibitory signals may play a role.

CAR activation can substitute for LFA-1 signaling

We further investigated how CAR signaling can overcome the dependence on LFA-1 for NK cell cytotoxicity. With the critical contribution of LFA-1 to trastuzumab-mediated degranulation already established, we took a step back and tested whether LFA-1 is required for initial conjugate formation between cancer cells and trastuzumab-armed or CAR-armed NK cells. We co-cultured labeled haNK cells combined with trastuzumab or NK-92/5.28.z cells with differentially labeled MDA-MB-453 cells in the presence or absence of LFA-1-blocking antibody. Both, haNK cells with trastuzumab and NK-92/5.28.z cells formed conjugates with MDA-MB-453 cells after 20 min of co-culture, without LFA-1 blockade resulting in a significant decrease in conjugation ability (figure 7A and B). Accordingly, we conclude that LFA-1 is not required for initial conjugate formation that precedes ADCC or CAR-mediated cell killing. We further tested whether granule polarization toward the immunological synapse in ADCC is affected by blockade of the LFA-1/ICAM-1 interaction. Our microscopy data showed that blockade of LFA-1 in haNK cells did not affect granule polarization toward the contact point with MDA-MB-453 cells in the presence of trastuzumab, suggesting that LFA-1 is rather required for the signaling leading to the subsequent release of cytotoxic granules (figure 7C and D). Hence, we further analyzed the signaling pathways downstream of LFA-1, FcγRIIIa and CAR. haNK cells were stimulated with immobilized trastuzumab, and NK-92/5.28.z cells with immobilized ErbB2, in each case in the presence or absence of immobilized anti-LFA-1. Then we measured phosphorylation of Pyk2 as a downstream signal after LFA-1 stimulation in

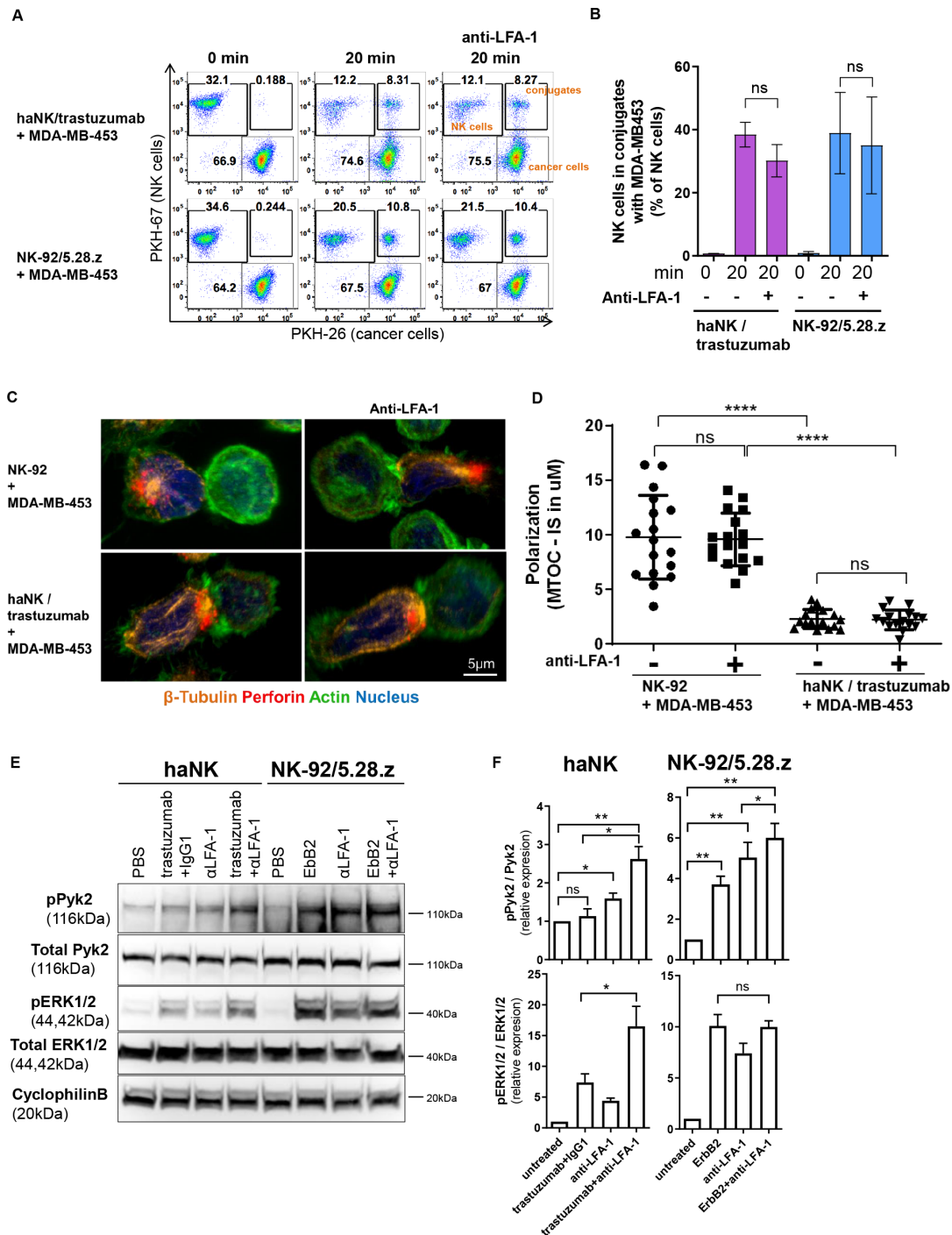


Figure 7 Chimeric antigen receptor activation can substitute for LFA-1 signaling by activating the Pyk2 pathway. (A) PKH-67-labeled haNK cells combined with trastuzumab or PKH-67-labeled NK-92/5.28.z cells were blocked with anti-LFA-1 antibody, and incubated with PKH-26-labeled MDA-MB-453 target cells for 20 min at 37°C as indicated. Control samples at 0 min were used to exclude unspecific binding or cross-staining. Cells were fixed and analyzed for conjugate formation by flow cytometry. (B) Quantification of conjugate formation. Pooled data from three independent experiments performed in triplicate are shown. Data represent mean values \pm SEM. (C) Confocal microscopy of NK-92 cells, and haNK cells combined with trastuzumab, incubated with MDA-MB-453 target cells. NK cells were blocked with anti-LFA-1 antibody prior to exposure to cancer cells as indicated. Representative images are shown. (D) Microtubule-organizing center (MTOC) polarization toward the immunological synapse (IS) was quantified from three independent experiments. Mean values \pm SEM are shown. (E) haNK or NK-92/5.28.z cells were stimulated with plate-bound trastuzumab, anti-LFA-1 antibody, ErbB2, or isotype control antibody as indicated. Cell lysates were prepared and analyzed by immunoblotting for phospho-Pyk2 (pPyk2; Tyr402) and phospho-ERK1/2 (pERK1/2; Thr202/Tyr204). As controls, total Pyk2 and ERK1/2 levels were analyzed. Cyclophilin B was used as a loading control. (F) Quantification of Pyk2 and ERK1/2 phosphorylation normalized to total protein levels. Data were pooled from three independent experiments. Mean values \pm SEM are shown. haNK, high-affinity Fc γ RIIIa-modified NK-92 cells; NK, natural killer; PBS, phosphate-buffered saline.

NK cells,³¹ and phosphorylation of ERK as an indicator of effective ADCC and CAR-mediated cytotoxicity.¹⁸ As expected, stimulation of LFA-1 alone resulted in Pyk2 phosphorylation in both, haNK and NK-92/5.28.z cells (figure 7E and F). Trastuzumab alone did not induce Pyk2 signaling via FcγRIIIa in haNK cells, whereas ErbB2 alone was sufficient to stimulate Pyk2 phosphorylation in NK-92/5.28.z cells. Combining anti-LFA-1 with ErbB2 further increased Pyk2 phosphorylation in NK-92/5.28.z cells, although to a limited extent (19%). In contrast, combination of trastuzumab and anti-LFA-1 resulted in a 64% increase in haNK cells. Consistent with our degranulation data, phosphorylation of ERK was only slightly induced in haNK cells by trastuzumab alone, while strong phosphorylation was observed after exposure to trastuzumab in combination with anti-LFA-1. Conversely, stimulation of the CAR in NK-92/5.28.z cells by ErbB2 was already sufficient for strong ERK phosphorylation, and was not increased further by additional LFA-1 activation. Taken together, these data demonstrate that CAR activation can substitute for LFA-1 signaling, and thus overcome immune escape based on ICAM-1 downregulation.

DISCUSSION

NK cells are increasingly recognized as promising and potent effectors for cancer immunotherapy. To enhance and specifically direct their cytotoxicity to tumor cells, NK cells can be combined with therapeutic antibodies such as trastuzumab, or genetically engineered with CAR constructs.^{18 28 32} Treatment regimens based on trastuzumab are standard of care for ErbB2-positive breast cancers. Nevertheless, some patients with breast cancer fail antibody therapy despite continued ErbB2 expression in their tumors, with the underlying mechanisms not yet fully understood.¹⁴ NK-mediated ADCC is considered to be important for trastuzumab efficacy, suggesting that escape of cancer cells from antibody-mediated NK cell cytotoxicity could contribute to treatment resistance. In an initial clinical trial, adoptive transfer of CD19-targeted CAR-NK cells has shown encouraging efficacy against B-cell malignancies.² Nevertheless, similar to CAR-T cells, CAR-NK cells employed for the treatment of solid tumors may face challenges such as inhomogeneous target antigen expression and an immunosuppressive tumor microenvironment. In addition, tumor cell-intrinsic resistance may affect ADCC and CAR-mediated cytotoxicity of NK cells despite sufficient target antigen expression. Hence, to fully exploit the potential of antibody-targeted and CAR-targeted NK cells for cancer immunotherapy, it is crucial to better understand escape of cancer cells from NK cell cytotoxicity, and to identify ways to overcome respective resistance mechanisms. In this study, we demonstrated for the first time that downregulation of ICAM-1 on breast and pancreatic cancer cells can abrogate trastuzumab-mediated NK cell cytotoxicity, while antitumor activity of CAR-NK cells remained unaffected.

ICAM-1 can be downregulated in cancer cells or cleaved by specific proteases.^{22–24} This has been shown to lead to escape from natural NK cell cytotoxicity,²⁵ which is triggered by activating receptors such as natural cytotoxicity receptors and NKG2D in response to stress-induced ligands on the tumor cell surface.³³ Accordingly, modulation of adhesion molecules constitutes a clinically relevant mechanism enabling cancer cells to evade attack by NK cells. Our data provide evidence that decrease or loss of ICAM-1 may also affect therapeutic efficacy of trastuzumab and possibly also other therapeutic antibodies. This is consistent with an earlier observation that cancer cells, which were experimentally kept under ADCC pressure, spontaneously downregulated ICAM-1.³⁴ Here, we showed that cancer cells with low ICAM-1 expression do not stimulate LFA-1 on NK cells, resulting in insufficient trastuzumab-induced ADCC. In addition, shedding of soluble ICAM-1 could result in blockade of LFA-1 and prevent its binding to membrane-anchored ICAM-1 on cancer cells.²² Hence, our data may have strong clinical implications with respect to trastuzumab therapy, and may at least in part explain why some patients do not respond to treatment. In this respect, it appears warranted to include analysis of ICAM-1 expression on cancer cells as a diagnostic parameter to enable correlative studies that investigate the relationship between ICAM-1 levels and clinical trastuzumab efficacy.

In the present study, we showed that 5AZA upregulates ICAM-1 expression and thereby prevents escape from trastuzumab-mediated NK cell cytotoxicity. 5AZA is a clinically approved drug for the treatment of myelodysplastic syndrome and AML, which may aid the development of 5AZA combination therapies with trastuzumab. Furthermore, also TNF- α and IFN- γ can increase ICAM-1 expression.^{26 30} In our experiments, IFN- γ and TNF- α were readily secreted by NK cells after trastuzumab-induced activation, but not when ICAM-1 was downregulated. Hence, 5AZA may be suitable to initially upregulate ICAM-1 on cancer cells, which would in turn enhance activation of NK cells, resulting in the secretion of IFN- γ and TNF- α , and in a positive loop further amplifying ICAM-1 levels. Likewise, other demethylating agents or ICAM-1 upregulating reagents may be tested for their potential to enhance antibody-dependent cytotoxicity of NK cells.

Recent data from CAR-T cell studies showed that sufficient ICAM-1 expression is critical for efficient antitumor activity of CAR-T cells.²⁶ To our surprise, we found that effective cell killing by CAR-NK cells targeting ErbB2 did not depend on ICAM-1, and was not affected by genetic KO of ICAM-1 in cancer cells or blockade of LFA-1 on the NK cells. Thereby, the CAR-NK cells could bypass ICAM-1-based escape in short-term and long-term cytotoxicity assays. Furthermore, in contrast to trastuzumab-stimulated NK cells, the secretion of critical cytokines and chemokines such as IFN- γ , TNF- α or MIP-1 α by the CAR-NK cells was not affected after contact with ICAM-1-negative cancer cells. Accordingly, CAR-NK cells can

provide robust anticancer functionality independent of stimulation by ICAM-1.

Our experiments with immobilized activating antibodies showed that trastuzumab alone is not able to stimulate degranulation of FcγRIIIa-positive NK cells, but requires additional stimulation of LFA-1. This is consistent with previous findings in insect cells using rabbit anti-serum that triggers the FcγRIIIa on human NK cells.²¹ In contrast, similar to our observations in cytotoxicity assays, CAR-activation by antigen was sufficient to induce degranulation without additional LFA-1 stimulation. Nevertheless, when the concentration of the CAR target antigen was decreased, ensuing suboptimal degranulation was rescued by additional LFA-1 activation. Accordingly, trastuzumab-mediated degranulation requires co-stimulation by LFA-1, while CAR-induced degranulation only requires additional signals if antigen concentration is low. In addition, degranulation induced by simultaneous FcγRIIIa and LFA-1 stimulation was still inhibited by NKG2A, whereas NKG2A had little effect on CAR-mediated NK cell activation. A previous report already described resistance of NK-92/5.28.z CAR-NK cells to inhibition by transforming growth factor-beta (TGF-β).³⁵ This suggests that CAR signaling in the NK cells is particularly strong, and difficult to override by inhibitory signaling pathways. Interestingly, our cytotoxicity studies with two HLA-E positive cancer cell types did not show improved ADCC or CAR-mediated cytotoxicity after NKG2A blockade. This suggests that although NKG2A can inhibit FcγRIIIa/LFA-1 NK cell activation, the situation in cell–cell interaction is more complex and additional inhibitory mechanisms might co-suppress NK cell cytotoxicity. In fact, the therapeutic anti-NKG2A antibody monalizumab showed improved natural NK cell cytotoxicity *in vitro* and *in vivo* and is currently under clinical evaluation.^{36–37} Interestingly, and in agreement with our cytotoxicity data, the combination of monalizumab and trastuzumab did not induce objective responses in patients with heavily pretreated HER2-positive breast cancer in a small cohort, while ICAM-1 expression levels on cancer cells were not investigated.³⁸ These data suggest that at least in some tumor types an additional mechanism may contribute to the inhibition of NK and T-cell responses. Further studies should address whether blockade of NKG2A can increase ADCC and thus therapeutic benefit. In fact, genetic KO of NKG2A expression has been shown to increase natural NK cell cytotoxicity against leukemic cells,³⁹ but whether disruption of the HLA-E/NKG2A checkpoint axis will improve CAR-NK cell cytotoxicity remains unclear. Based on our findings, we propose screening patient tumors for ICAM-1 expression, as this may influence the ADCC response in combination with tumor-specific therapeutic antibodies.

In addition to our models with MDA-MB-453 breast cancer cells, the sensitivity of trastuzumab-triggered ADCC and resistance of CAR-mediated cytotoxicity to LFA-1 blockade was confirmed with other breast and pancreatic cancer cells. Likewise, unmodified and CAR-engineered

primary human NK cells from peripheral blood demonstrated the same dependence on LFA-1 for effective trastuzumab-induced ADCC and LFA-1-independence on CAR-activation as respective haNK and NK-92/5.28.z cells. This demonstrates the robustness and general validity of our findings, which will likely be relevant also for therapeutic antibodies and CAR-NK cells targeting antigens other than ErbB2. However, it is important to note that this study is limited as it has been conducted *in vitro* only. Therefore next studies are required to further validate the role of the ICAM-1/LFA-1 axis in preclinical models and in primary tumors from patients responding and non-responding to trastuzumab treatment.

It would also be interesting to test whether other attempts to improve targeted NK cell therapy can synergize with our findings, such as targeting TGF-β signaling or improved metabolic activity by CIS (cytokine-inducible SH2-containing protein) KO, expression of transgenic cytokines such as interleukin-15, and many others.^{40–43}

In recent years, different approaches have been developed to enhance NK cell cytotoxicity and facilitate targeted antitumor activity. NK cells have been modified with chimeric CD64/CD16A Fc receptors, or combined with bispecific or trispecific killer cell engagers such as bispecific antibodies cross-linking tumor antigens with FcγRIIIa (CD16) or NKG2D, or tetraspecific ANKET molecules.^{44–49} In addition, NK cells carrying a universal CAR have been developed, which can be targeted to a tumor antigen of choice by combining them with a respective bispecific adaptor molecule.^{50–51} Further research appears justified to investigate whether these therapeutic strategies like classical ADCC are affected by ICAM-1 downregulation, or can overcome this resistance mechanism similar to NK cells engineered with a conventional CAR. Recently, FcγRIIIa-expressing haNK cells have been further modified to also express a tumor-targeting CAR (t-haNK cells).⁵² In the context of our findings, this approach may benefit from both, the flexibility to induce ADCC by combination with different therapeutic antibodies, and the CAR-dependent resistance to inhibition by ICAM-1 downregulation.

High-resolution analysis of the immunological synapse with TIRF microscopy revealed that CAR-NK cells do not recruit ICAM-1 molecules to the immunological synapse. In contrast, NK cells combined with trastuzumab recruited ICAM-1, and formed typical pSMAC structures. Nevertheless, how ICAM-1 molecules are excluded from the immunological synapse of CAR-NK cells is unclear at present, and requires further investigation.

LFA-1 plays multiple roles in NK cells, including intercellular adhesion and signal transduction.¹⁹ Our data suggest that its contribution to cell–cell adhesion is not relevant for trastuzumab-mediated or CAR-mediated targeting of NK cells. Presumably, the interaction with target cells via trastuzumab and FcγRIIIa or the CAR is already strong enough, and LFA-1 does not provide any additional benefit. We also showed that the ICAM-1/LFA-1 interaction does not affect granule polarization toward the

immunological synapse, suggesting that a different mechanism is involved in ICAM-1-based resistance of ICAM-1^{low} cells to trastuzumab-mediated ADCC. Instead, our data demonstrate that LFA-1 is rather required to provide critical molecular signals for ADCC, which is consistent with earlier data obtained with insect target cells.^{31–53} In our case, activation of Pyk2 signaling via LFA-1 was essential for trastuzumab-mediated ADCC, with FcγRIIIa stimulation alone unable to activate this pathway. In contrast, CAR-activation resulted in Pyk2 phosphorylation in NK cells independent of LFA-1, providing a mechanistic explanation for the observation that functionality of CAR-NK cells was not affected by ICAM-1 downregulation on cancer cells. At the same time, we showed that during both, FcγRIIIa/LFA-1 and CAR-based signaling, Pyk2 phosphorylation correlated with the phosphorylation of ERK1/2, which is an important downstream NK cell signaling molecule leading to NK cell activation and cytotoxicity.⁵⁴ It has been shown by others that ERK1/2 is one of the downstream signaling pathways of Pyk2, suggesting that FcγRIIIa/LFA-1 or CAR-mediated phosphorylation of Pyk2 contributes to downstream NK cell activation signals through ERK1/2-mediated signaling.^{55–56} Further research is needed to elucidate these complex molecular signaling pathways in antibody-targeted and CAR-targeted NK cells in order to improve NK cell-based therapies. Importantly, in our study we tested one of the most widely used CAR signaling molecules based on CD3z and CD28 stimulation, but recently novel CAR signaling molecules have been introduced to replace classical T cell-based signaling modules to enhance NK cell cytotoxicity,^{57–58} and it would be clinically relevant to test whether these novel CARs are dependent on ICAM-1 expression on cancer cells and which signaling pathways are employed.

CONCLUSION

Our study clearly demonstrates that ICAM-1 is an important checkpoint in trastuzumab-mediated NK cell cytotoxicity. Hence, cancer cells that downregulate or shed ICAM-1 are more likely to escape trastuzumab treatment. In sharp contrast, CAR-NK cells targeting the same tumor antigen remained unaffected by ICAM-1 downregulation or loss of LFA-1 stimulation. Mechanistically, the distinct signaling properties of FcγRIIIa and CAR can explain this difference. CAR-activation can substitute for LFA-1-mediated Pyk2 signaling and rescue NK cell degranulation, cytotoxicity and cytokine release that is otherwise abrogated on encounter of ICAM-1^{low} or ICAM-1-negative cancer cells. Accordingly, for the treatment of ErbB2-positive but ICAM-1^{low} breast cancers a combination of trastuzumab with ICAM-1 upregulating drugs like 5AZA, or application of ErbB2-specific CAR-NK cells may be warranted. Future studies will be aimed at investigating whether the same mechanisms apply to therapeutic antibodies and CAR-NK cells targeting tumor antigens other than ErbB2, as well as to alternative targeting approaches based on bispecific NK cell engagers and modular CAR

systems. This is expected to provide more comprehensive insights in ICAM-1-based immune escape, which will be relevant for the development of further refined and more effective NK cell therapies.

Author affiliations

- ¹Experimental Transfusion Medicine, Faculty of Medicine Carl Gustav Carus, Dresden University of Technology, Dresden, Germany
- ²Institute for Transfusion Medicine Dresden, German Red Cross Blood Donation Service North-East, Dresden, Germany
- ³German Cancer Consortium (DKTK), Partner Site Dresden, Dresden, Germany
- ⁴Medical University of Vienna, Center for Pathophysiology, Infectiology and Immunology, Institute for Hygiene and Applied Immunology, Vienna, Austria
- ⁵TU Dresden, Medical Faculty and University Hospital Carl Gustav Carus, Department of Neurosurgery, Division of Experimental Neurosurgery and Tumor Immunology, Dresden, Germany
- ⁶German Cancer Consortium (DKTK), partner site Dresden, Germany; German Cancer Research Center (DKFZ), Heidelberg, Germany, National Center for Tumor Diseases (NCT), Dresden, Germany
- ⁷Institute of Radiopharmaceutical Cancer Research, Helmholtz-Zentrum Dresden-Rossendorf, Dresden, Germany
- ⁸National Center for Tumor Diseases Dresden (NCT/UCC), Dresden, Germany
- ⁹ImmunityBio Inc, Culver City, California, USA
- ¹⁰Georg-Speyer-Haus, Institute for Tumor Biology and Experimental Therapy, Frankfurt am Main, Germany
- ¹¹Frankfurt Cancer Institute, Goethe University, Frankfurt am Main, Germany
- ¹²German Cancer Consortium (DKTK), Partner Site Frankfurt/Mainz, a partnership between DKFZ and University Hospital Frankfurt, Frankfurt am Main, Germany

Acknowledgements The authors thank Erik Zenker and Madeleine Teichert for outstanding technical assistance, Silke Tulok for excellent support with light microscopy, and Professor Peter Fasching for helpful discussions. BioRender software was used to generate the illustrations in the graphical abstract.

Contributors Designing of research studies: JE, TT. Conducting experiments: JE, WR, NW, VG, NMS, AS, PO-M, LRL, SM. Acquiring data: JE, WR, NW, VG, NMS, AS, CO, LRL. Analyzing data: JE, WR, VG, NMS, AS, LRL. Writing the manuscript: JE, TT, WSW, LB, HK, JBH, AF, MB, SRK, AT. Study supervision: JE, TT. All authors read and approved the final version of the manuscript.

Funding This research was supported in part by the German Research Foundation (DFG) through grant EI1223/2-1 to JE; German Federal Ministry of Education and Research (Clusters4Future SaxoCell, 03ZU1111DA) and German Red Cross Blood Donation Service internal grants to TT; Innovative Medicines Initiative 2 Joint Undertaking under grant agreement No 116026 (T2EVOLVE) to VG and JBH.

Competing interests TT and WSW are named as inventors on patents in the field of cancer immunotherapy owned by their respective institutions. HK and LB are employed by ImmunityBio, California, USA. Other authors declare that they have no competing interests.

Patient consent for publication Not applicable.

Ethics approval This study does not involve human participants.

Provenance and peer review Not commissioned; externally peer reviewed.

Data availability statement All data relevant to the study are included in the article or uploaded as supplementary information. Further inquiries can be directed to the corresponding author.

Supplemental material This content has been supplied by the author(s). It has not been vetted by BMJ Publishing Group Limited (BMJ) and may not have been peer-reviewed. Any opinions or recommendations discussed are solely those of the author(s) and are not endorsed by BMJ. BMJ disclaims all liability and responsibility arising from any reliance placed on the content. Where the content includes any translated material, BMJ does not warrant the accuracy and reliability of the translations (including but not limited to local regulations, clinical guidelines, terminology, drug names and drug dosages), and is not responsible for any error and/or omissions arising from translation and adaptation or otherwise.

Open access This is an open access article distributed in accordance with the Creative Commons Attribution Non Commercial (CC BY-NC 4.0) license, which permits others to distribute, remix, adapt, build upon this work non-commercially, and license their derivative works on different terms, provided the original work is

properly cited, appropriate credit is given, any changes made indicated, and the use is non-commercial. See <http://creativecommons.org/licenses/by-nc/4.0/>.

ORCID iDs

Jiri Eitler <http://orcid.org/0000-0002-3175-2438>
 Johannes B Huppa <http://orcid.org/0000-0003-2634-8198>
 Winfried S Wels <http://orcid.org/0000-0001-9858-3643>
 Torsten Tonn <http://orcid.org/0000-0001-9580-2193>

REFERENCES

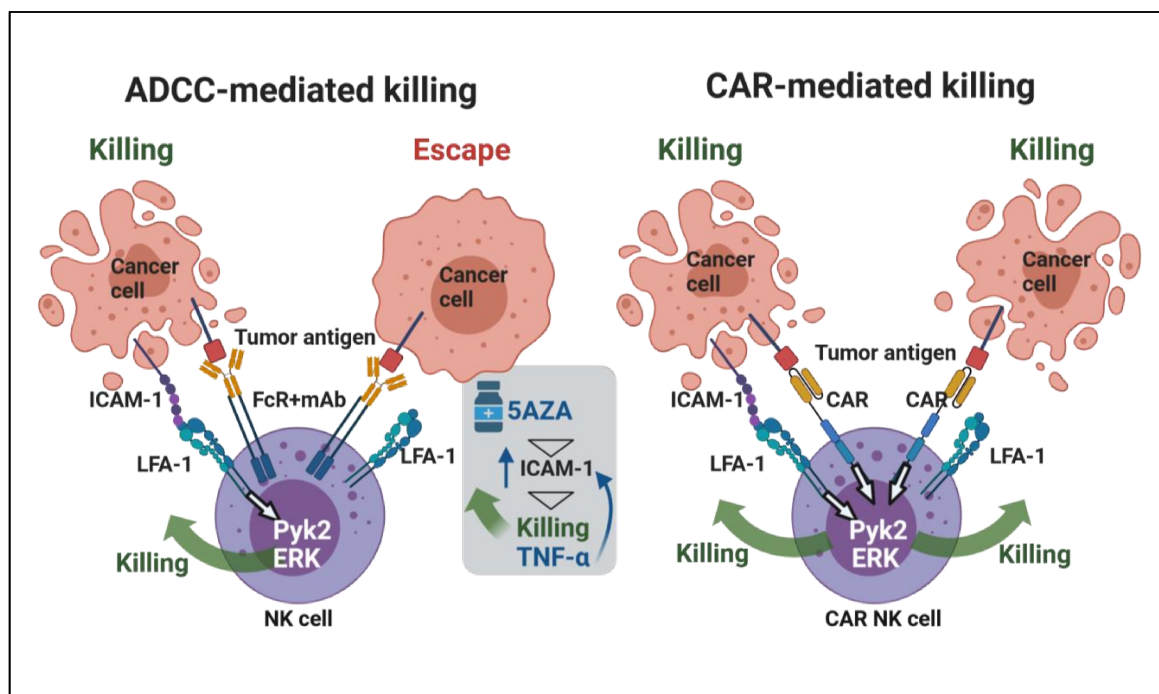
- Myers JA, Miller JS. Exploring the NK cell platform for cancer immunotherapy. *Nat Rev Clin Oncol* 2021;18:85–100.
- Liu E, Marin D, Banerjee P, et al. Use of CAR-Transduced natural killer cells in Cd19-positive Lymphoid tumors. *N Engl J Med* 2020;382:545–53.
- Zhu H, Lai YS, Li Y, et al. Concise review: human pluripotent stem cells to produce cell-based cancer immunotherapy. *Stem Cells* 2018;36:134–45.
- Miller JS, Soignier Y, Panoskaltis-Mortari A, et al. Successful adoptive transfer and in vivo expansion of human haploidentical NK cells in patients with cancer. *Blood* 2005;105:3051–7.
- Tonn T, Schwabe D, Klingemann HG, et al. Treatment of patients with advanced cancer with the natural killer cell line NK-92. *Cytotherapy* 2013;15:1563–70.
- Tonn T, Becker S, Esser R, et al. Cellular immunotherapy of malignancies using the clonal natural killer cell line NK-92. *J Hematother Stem Cell Res* 2001;10:535–44.
- Watzl C, Long EO. Signal transduction during activation and inhibition of natural killer cells. *Curr Protoc Immunol* 2010;11.
- Retecki K, Seweryn M, Graczyk-Jarzynka A, et al. The immune landscape of breast cancer: strategies for overcoming Immunotherapy resistance. *Cancers (Basel)* 2021;13:6012.
- Romanski A, Bug G, Becker S, et al. Mechanisms of resistance to natural killer cell-mediated cytotoxicity in acute lymphoblastic leukemia. *Exp Hematol* 2005;33:344–52.
- Maki G, Hayes GM, Naji A, et al. NK resistance of tumor cells from multiple myeloma and chronic lymphocytic leukemia patients: implication of HLA-G. *Leukemia* 2008;22:998–1006.
- Hasenkamp J, Borgerding A, Wulf G, et al. Resistance against natural killer cell cytotoxicity: analysis of mechanisms. *Scand J Immunol* 2006;64:444–9.
- Jochems C, Hodge JW, Fantini M, et al. An NK cell line (haNK) expressing high levels of granzyme and engineered to express the high affinity Cd16 allele. *Oncotarget* 2016;7:86359–73.
- Maadi H, Soheilifar MH, Choi W-S, et al. Trastuzumab mechanism of action; 20 years of research to unravel a dilemma. *Cancers (Basel)* 2021;13:3540.
- Arnould L, Gelly M, Penault-Llorca F, et al. Trastuzumab-based treatment of Her2-positive breast cancer: an antibody-dependent cellular cytotoxicity mechanism *Br J Cancer* 2006;94:259–67.
- Karvouni M, Vidal-Manrique M, Lundqvist A, et al. Engineered NK cells against cancer and their potential applications beyond. *Front Immunol* 2022;13.
- Finck AV, Blanchard T, Roselle CP, et al. Engineered cellular Immunotherapies in cancer and beyond. *Nat Med* 2022;28:678–89.
- Burger MC, Forster M-T, Romanski A, et al. Intracranial injection of NK cells engineered with a Her2-targeted chimeric antigen receptor in patients with recurrent glioblastoma. *Neuro Oncol* 2023;25:2058–71.
- Eitler J, Wotschel N, Miller N, et al. Inability of granule polarization by NK cells defines tumor resistance and can be overcome by CAR or ADCC mediated targeting. *J Immunother Cancer* 2021;9:e001334.
- Urlaub D, Höfer K, Müller M-L, et al. LFA-1 activation in NK cells and their subsets: influence of receptors, maturation, and cytokine stimulation. *J Immunol* 2017;198:1944–51.
- Mentlik AN, Sanborn KB, Holzbaur EL, et al. Rapid lytic granule convergence to the MTOC in natural killer cells is dependent on dynein but not cytolytic commitment. *Mol Biol Cell* 2010;21:2241–56.
- Hsu H-T, Mace EM, Carisey AF, et al. NK cells converge lytic granules to promote cytotoxicity and prevent bystander killing. *J Cell Biol* 2016;215:875–89.
- Becker JC, Dummer R, Hartmann AA, et al. Shedding of ICAM-1 from human melanoma cell lines induced by IFN-gamma and tumor necrosis factor-alpha. functional consequences on cell-mediated cytotoxicity. *J Immunol* 1991;147:4398–401.
- Hamai A, Meslin F, Benlalam H, et al. ICAM-1 has a critical role in the regulation of metastatic melanoma tumor susceptibility to CTL lysis by interfering with PI3K/AKT pathway. *Cancer Res* 2008;68:9854–64.
- Ueda R, Kohanbash G, Sasaki K, et al. Dicer-regulated microRNAs 222 and 339 promote resistance of cancer cells to cytotoxic T-lymphocytes by down-regulation of ICAM-1. *Proc Natl Acad Sci U S A* 2009;106:10746–51.
- Xiao Y, Chen J, Wang J, et al. Acute myeloid leukemia epigenetic immune escape from nature killer cells by ICAM-1. *Front Oncol* 2021;11.
- Larson RC, Kann MC, Bailey SR, et al. CAR T cell killing requires the IFNγR pathway in solid but not liquid tumours. *Nature* 2022;604:563–70.
- Maki G, Klingemann HG, Martinson JA, et al. Factors regulating the cytotoxic activity of the human natural killer cell line, NK-92. *J Hematother Stem Cell Res* 2001;10:369–83.
- Schönfeld K, Sahn C, Zhang C, et al. Selective inhibition of tumor growth by clonal NK cells expressing an Erbb2/Her2-specific Chimeric antigen receptor. *Mol Ther* 2015;23:330–8.
- Murphy A, Long A, Volkov Y, et al. Cross-linking of LFA-1 induces secretion of macrophage inflammatory protein (MIP)-1alpha and MIP-1beta with consequent directed migration of activated lymphocytes. *Eur J Immunol* 2000;30:3006–11.
- Wu T, Shi J-X, Geng S, et al. The Mk2/Hur signaling pathway regulates TNF-A-induced ICAM-1 expression by promoting the stabilization of ICAM-1 mRNA. *BMC Pulm Med* 2016;16:84.
- Zhang M, March ME, Lane WS, et al. A signaling network stimulated by beta2 integrin promotes the polarization of lytic granules in cytotoxic cells. *Sci Signal* 2014;7.
- Uherek C, Tonn T, Uherek B, et al. Retargeting of natural killer-cell cytolytic activity to erbb2-expressing cancer cells results in efficient and selective tumor cell destruction. *Blood* 2002;100:1265–73.
- Vivier E, Tomasello E, Baratin M, et al. Functions of natural killer cells. *Nat Immunol* 2008;9:503–10.
- Aldeghaither DS, Zahavi DJ, Murray JC, et al. A mechanism of resistance to antibody-targeted immune attack. *Cancer Immunol Res* 2019;7:230–43.
- Zhang C, Burger MC, Jennewein L, et al. Erbb2/Her2-specific NK cells for targeted therapy of glioblastoma. *J Natl Cancer Inst* 2016;108.
- André P, Denis C, Soulas C, et al. Anti-Nkg2A mAb is a checkpoint inhibitor that promotes anti-tumor immunity by unleashing both T and NK cells. *Cell* 2018;175:1731–1743.
- Herbst RS, Majem M, Barlesi F, et al. COAST: an open-label, phase II, multidrug platform study of durvalumab alone or in combination with oleclumab or monalizumab in patients with unresectable, stage III non-small-cell lung cancer. *JCO* 2022;40:3383–93.
- Geurts VCM, Voorwerk L, Balduzzi S, et al. Unleashing NK- and Cd8 T cells by combining monalizumab and trastuzumab for metastatic Her2-positive breast cancer: results of the MIMOSA trial. *Breast* 2023;70:76–81.
- Bexte T, Alzubi J, Reindl LM, et al. CRISPR-Cas9 based gene editing of the immune checkpoint Nkg2A enhances NK cell mediated cytotoxicity against multiple myeloma. *Oncimmunology* 2022;11.
- Delconte RB, Kolesnik TB, Dagley LF, et al. CIS is a potent checkpoint in NK cell-mediated tumor immunity. *Nat Immunol* 2016;17:816–24.
- Liu E, Tong Y, Dotti G, et al. Cord blood NK cells engineered to express IL-15 and a Cd19-targeted CAR show long-term persistence and potent antitumor activity. *Leukemia* 2018;32:520–31.
- Silvestre RN, Eitler J, de Azevedo JTC, et al. Engineering NK-CAR.19 cells with the IL-15/IL-15alpha complex improved proliferation and anti-tumor effect in vivo. *Front Immunol* 2023;14.
- Chaudhry K, Geiger A, Dowlati E, et al. Co-transducing B7H3 CAR-NK cells with the DNR preserves their cytolytic function against GBM in the presence of exogenous TGF-beta. *Mol Ther Methods Clin Dev* 2022;27:415–30.
- Snyder KM, Hullsiek R, Mishra HK, et al. Expression of a recombinant high affinity IgG FC receptor by engineered NK cells as a docking platform for therapeutic mAbs to target cancer cells. *Front Immunol* 2018;9.
- Demaria O, Gauthier L, Vetzou M, et al. Antitumor immunity induced by antibody-based natural killer cell engager therapeutics armed with not-alpha IL-2 variant. *Cell Rep Med* 2022;3:100783.
- Wingert S, Reusch U, Knackmuss S, et al. Preclinical evaluation of Afm24, a novel Cd16A-specific innate immune cell engager targeting EGFR-positive tumors. *Mabs* 2021;13.
- Vallera DA, Oh F, Kodali B, et al. A Her2 tri-specific NK cell engager mediates efficient targeting of human ovarian cancer. *Cancers (Basel)* 2021;13.
- Pinto S, Pahl J, Schottelius A, et al. Reimagining antibody-dependent cellular cytotoxicity in cancer: the potential of natural killer cell engagers. *Trends Immunol* 2022;43:932–46.



- 49 Zhang C, Röder J, Scherer A, *et al.* Bispecific antibody-mediated Redirection of Nkg2D-CAR natural killer cells facilitates dual targeting and enhances antitumor activity. *J Immunother Cancer* 2021;9:10.
- 50 Mitwasi N, Feldmann A, Arndt C, *et al.* Unicar-modified off-the-shelf NK-92 cells for targeting of Gd2-expressing tumour cells. *Sci Rep* 2020;10:2141.
- 51 Pfeifer Serrahima J, Zhang C, Oberoi P, *et al.* Multivalent adaptor proteins specifically target NK cells carrying a universal chimeric antigen receptor to Erbb2 (Her2)-expressing cancers. *Cancer Immunol Immunother* 2023;72:2905–18.
- 52 Fabian KP, Padget MR, Donahue RN, *et al.* PD-L1 targeting high-affinity NK (t-haNK) cells induce direct antitumor effects and target suppressive MDSC populations. *J Immunother Cancer* 2020;8:e000450.
- 53 March ME, Long EO. Beta2 integrin induces tcrzeta-syk-phospholipase C-gamma phosphorylation and paxillin-dependent granule polarization in human NK cells. *J Immunol* 2011;186:2998–3005.
- 54 Chen X, Trivedi PP, Ge B, *et al.* Many NK cell receptors activate Erk2 and Jnk1 to trigger microtubule organizing center and granule polarization and cytotoxicity. *Proc Natl Acad Sci USA* 2007;104:6329–34.
- 55 Selitrennik M, Lev S. Pyk2 integrates growth factor and cytokine receptors signaling and potentiates breast cancer invasion via a positive feedback loop. *Oncotarget* 2015;6:22214–26.
- 56 Zhu X, Bao Y, Guo Y, *et al.* Proline-rich protein tyrosine kinase 2 in inflammation and cancer. *Cancers (Basel)* 2018;10:139.
- 57 Li Y, Hermanson DL, Moriarity BS, *et al.* Human iPSC-derived natural killer cells engineered with chimeric antigen receptors enhance anti-tumor activity. *Cell Stem Cell* 2018;23:181–92.
- 58 Töpfer K, Cartellieri M, Michen S, *et al.* Dap12-based activating chimeric antigen receptor for NK cell tumor immunotherapy. *J Immunol* 2015;194:3201–12.

CAR-mediated Targeting of NK Cells Overcomes Tumor Immune Escape Caused by ICAM-1 Downregulation

Graphical Abstract



Authors

Jiri Eitler, Wiebke Rackwitz, Natalie Wotschel, ..., Hans G. Klingemann, Winfried S. Wels, Torsten Tonn

Correspondence

j.eitler@blutspende.de

t.tonn@blutspende.de

Highlights

- ICAM-1 downregulation is a critical escape mechanism from trastuzumab-mediated NK cell cytotoxicity (ADCC).
- 5AZA treatment and TNF- α production restore trastuzumab-mediated NK cell cytotoxicity.
- CAR-NK cell cytotoxicity is independent of ICAM-1 levels by bypassing LFA-1 signaling through the Pyk2 and ERK1/2 pathway.

1 **Supplementary Materials for**
2 **CAR-mediated Targeting of NK Cells Overcomes Tumor Immune Escape**
3 **Caused by ICAM-1 Downregulation**

4 Jiri Eitler, Wiebke Rackwitz, Natalie Wotschel, Venugopal Gudipati, Nivedha Murali Shankar,
5 Anastasia Sidorenkova, Johannes B. Huppa, Paola Ortiz-Montero, Corinna Opitz, Stephan R.
6 Künzel, Susanne Michen, Achim Temme, Liliana R. Loureiro, Anja Feldmann, Michael
7 Bachmann, Laurent Boissel, Hans G. Klingemann, Winfried S. Wels, Torsten Tonn

8
9 **Document includes:**

10 Supplementary methods

11 Supplementary figures

12 Supplementary references

13 **SUPPLEMENTARY METHODS**

14

15 **Cells and cell culture**

16 The established human NK cell line NK-92 was kindly provided by Hans G. Klingemann (Vancouver,
17 Canada) (1). NK-92/5.28.z cells engineered with ErbB2-specific CAR were previously generated as
18 described (2). NK-92-derived haNK cells, engineered to express FcγRIIIa and IL-2, were kindly provided
19 by ImmunityBio, Inc. (Culver City, CA, USA) (3). NK cell lines were cultured in X-VIVO 10 medium
20 (Lonza) containing 5% heat-inactivated human AB plasma (German Red Cross Blood Donation Service
21 North-East, Dresden, Germany), 100 IU/mL penicillin, and 100 µg/mL streptomycin (Merck/Biochrom).
22 NK-92 and NK-92/5.28.z cells were additionally supplemented with 500 IU/mL IL-2 (Proleukin; Novartis
23 Pharma), referred to as complete X-VIVO 10 medium.

24 K562, MDA-MB-453, BxPc3, HEK293, and MCF-7 cells were purchased from the American Type
25 Culture Collection (ATCC; Manassas, VA, USA). HT18584-HLA-E*spG cells, with stable expression of
26 disulfide-stabilized HLA-E trimer consisting of β2-microglobulin, VMAPRTLFL-peptide and HLA-
27 E*01:03 ectodomain, has been previously described (4).

28 K562 cells were cultured in RPMI 1640 (Merck/Biochrom) supplemented with 10% heat-inactivated fetal
29 bovine serum (HI-FBS; Merck/Biochrom), 2 mM L-glutamine (Merck/Biochrom), 1 mM non-essential
30 amino acids (Merck/Biochrom), 1 mM sodium pyruvate (Merck/Biochrom), 100 IU/mL penicillin, and
31 100 µg/mL streptomycin. MDA-MB-453, BxPc3, HEK293, MCF-7 and HT18584-HLA-E*spG cells were

32 cultured in DMEM medium (Merck/Biochrom) supplemented with 10% HI-FBS, 2 mM L-glutamine, 100
33 IU/mL penicillin, and 100 µg/mL streptomycin. Medium for MCF-7 cells was additionally supplemented
34 with 10 µg/mL insulin (Sigma-Aldrich).

35 Human primary NK cells were isolated from healthy donors in accordance with the guidelines approved
36 by the local ethics committee. Peripheral blood mononuclear cells (PBMCs) were obtained by Biocoll
37 density centrifugation (Biochrom), and NK cells were isolated from PBMCs by negative selection using
38 the NK cell isolation kit according to the manufacturer's instructions (Miltenyi Biotec). Isolated NK cells
39 were cultured in NK MACS medium (Miltenyi Biotec) supplemented with 5% human AB serum (German
40 Red Cross Blood Donation Service North-East, Dresden, Germany), 1000 IU/mL IL-2 and 20 ng/mL IL-
41 21 (Miltenyi Biotec).

42 All cells were cultured at 37°C in a humidified atmosphere with 5% CO₂ and routinely checked for
43 *Mycoplasma* contamination.

44

45 **Flow cytometry**

46 Cells were stained for 30 min on ice with antibodies specific for ErbB2 (191924; R&D Systems), CD16
47 (3G8), LFA-1 (HI111), ICAM-1 (HA58), ICAM-2 (CBR-IC2/2), ICAM-3 (TU41) (all from BD
48 Biosciences) and HLA-E (3D12HLA-E), Thermofisher Scientific and ErbB2 (REA1232) from Miltenyi
49 Biotec. ErbB2-CAR detection was performed as previously described (5). Live cells were discriminated
50 using 7-AAD (BD Biosciences). Samples were acquired using a BD FACSCanto II flow cytometer and
51 data were analyzed using FlowJo software version 9 (BD Biosciences).

52 **Lentiviral transduction**

53 ICAM-1 knock out cell lines were generated by lentiviral transduction with a Cas9-expressing vector
54 (LentiCas9-Blast) followed by transduction with LentiGuide-Puro (both constructs were a gift from Feng
55 Zhang; (6)) containing gRNA targeting ICAM-1 with the following sequence 5'-
56 GCTATTCAAACCTGCCCTGAT-3'. Lentiviral particles were produced in HEK293T cells as packaging
57 cell line with packaging vectors psPAX2 and pMD2.G. Plasmids were transfected with polyethyleneimine
58 (PEI; Sigma-Aldrich), and supernatants were harvested after 48 hours. Viral particles were concentrated
59 with PEG-it solution (System Biosciences) according to the manufacturer's instructions. Lentiviral
60 transduction was performed at an MOI<1 by 30 min spinoculation at 1000 x g in the presence of 8 µg/mL
61 Polybrene (Sigma-Aldrich). Human primary NK cells isolated as described above were activated with NK
62 Cell Activation/Expansion Kit (Miltenyi) according to the manufacturer's protocol and transduced with
63 ErbB2-CAR-encoding lentiviral vector (2) at an MOI=10 after 4 days by 60 min spinoculation at 1000 x g
64 in the presence of 8 µg/mL Polybrene and 2.5 µM BX795 (InvivoGen). CAR expression was confirmed

65 by flow cytometry 72 hours after transduction, cells were expanded and used for experiments 7-14 days
66 after transduction. CAR expression and NK cell purity were analyzed at the time of the experiment.

67 **Europium-TDA (EuTDA) cytotoxicity assay**

68 Specific cytotoxicity of NK-92 cell lines against target cells was determined using an Europium (EuTDA)
69 cytotoxicity assay (DELFI, PerkinElmer) according to the manufacturer's protocol. Briefly, target cells
70 were loaded with an acetoxymethyl ester of the fluorescence-enhancing ligand (BATDA; Perkin Elmer)
71 and then co-incubated in triplicates at 10,000 cells/well with effector cells with or without trastuzumab
72 (Herceptin; 2 µg/mL; Roche) at the indicated E:T ratios. For blocking studies, NK cells were incubated
73 with blocking antibodies prior to mixing with cancer cells as described below. After 2 hours of co-culture,
74 supernatants were collected for measurement of the fluorescent signal reflecting target cell lysis using a
75 VICTOR X4 fluorometer (PerkinElmer). Specific lysis was calculated according to the standard formula.

$$\% \text{ Specific release} = \frac{\text{Experimental release (counts)} - \text{Spontaneous release (counts)}}{\text{Maximum release (counts)} - \text{Spontaneous release (counts)}} \times 100$$

76

77 **Treatment with 5-Aza-2'-deoxycytidine and TNF-α**

78 HEK293 cells were treated with 5-Aza-2'-deoxycytidine (5AZA; 1 µM; Selleckchem) for 72 hours or
79 TNF-α (100 ng/mL; Thermofisher Scientific) for 48 hours, washed, analyzed by flow cytometry and used
80 for cytotoxicity assays.

81 **Live cell imaging cytotoxicity assays**

82 Live cell imaging cytotoxicity assays were performed using the IncuCyte S3 instrument (Sartorius)
83 according to the manufacturer's protocol. Briefly, target cells were labeled with Cytolight Red reagent
84 (Sartorius), and 1*10⁴ cells per well were plated in triplicates in a poly-L-ornithine (Sigma-Aldrich)-
85 coated 96-well plate and incubated for 90 min at 37°C. Next, NK cells were added at a 1:1 E:T ratio.
86 Where indicated, trastuzumab (Herceptin; 5 µg/mL; Roche) was added. For blocking experiments, NK
87 cells were pre-incubated with anti-LFA-1 or anti-NKG2A antibody (20 µg/mL; TS1/22; Thermofisher) for
88 60 min at 37°C. Cells were co-cultured in complete X-VIVO 10 medium in the presence of Cytotox Green
89 (Sartorius) viability dye for 50 hours. Lysis was calculated as the percentage of dead target cells out of all
90 target cells. Data were analyzed using IncuCyte software and normalized to the baseline. Alternatively,
91 SKOV-3 cells were stably transduced with Nuclight Red fluorescent protein (Sartorius) and cytotoxicity
92 was measured by plotting fluorescence area over time.

93 **Blocking experiments**

94 For blocking experiments, NK cells were pre-incubated with antibodies at a concentration of 20 µg/mL for
95 60 min at 37°C. The following antibodies were used: anti-LFA-1 (TS1/22; Thermofisher), anti-NKG2D

96 (1D11; BD Biosciences), anti-DNAM-1 (102511; R&D Systems), anti-NKp30 (P30-15; Biolegend), anti-
97 NKp44 (44.189; Thermofisher), anti-NKp46 (9E2; Thermofisher), anti-2B4 (PP35; Thermofisher), anti-
98 NKG2A (Z199; Beckman Coulter), IgG1 (107.3; BD Biosciences) and IgG2b (MPC-11; Biolegend).

99 **Cytokine measurements**

100 NK and cancer cells were co-cultured in duplicates in complete X-VIVO-10 medium at an E:T ratio of 1:1
101 at a density of 5×10^5 cells/mL for each cell type. Where indicated, NK cells were blocked with anti-LFA-1
102 antibody (20 μ g/mL; TS1/22; Thermofisher). After 6 hours, the cells were spun down and the supernatant
103 was used for cytokine measurements using the Luminex assay (Procartaplex, Thermofisher) according to
104 the manufacturer's protocols. Measurements were performed on the Luminex Flexmap 3D system.

105 **Degranulation assay**

106 Flat-bottom 96-well plates were coated with antibodies or recombinant proteins at a concentration of 10
107 μ g/mL for 60 min at 37°C. The wells were then washed 2x with PBS and finally aspirated. NK cells
108 prepared in complete X-VIVO-10 medium without IL-2, and 1×10^5 cells were added to each well in
109 duplicates. Cells were incubated in the coated plates for 2 hours at 37°C in the presence of CD107a
110 antibody (eBioH4A3; Invitrogen). Degranulation was stopped by transferring the plate to ice. The cells
111 were harvested and analyzed by flow cytometry. The following antibodies and recombinant proteins were
112 used for plate coating: anti-LFA-1 (TS1/22; Thermofisher), anti-NKG2A (Z199; Beckman Coulter), anti-
113 PD-1 (MIH4; BD Biosciences), anti-TIGIT (MBSA43; Thermofisher), anti-Tim3 (F38-2E2; Biolegend),
114 trastuzumab, human recombinant ErbB2-Fc (R&D Systems). Controls were coated with IgG1 (107.3; BD
115 Biosciences), IgG2b (MPC-11; Biolegend) or human HSA (Baxter).

116 **Western blot**

117 NK cells were rested in X-VIVO 10 medium without supplements for 60 min at 37°C and then transferred
118 on ice to 96-well plates coated with antibodies or recombinant proteins. Coated plates were prepared as for
119 the degranulation assay. After 20 min of activation at 37°C, cells were lysed by adding RIPA lysis buffer
120 (Cell Signaling) containing protease and phosphatase inhibitor cocktails (Roche). Samples were mixed
121 thoroughly, and incubated for 20 min on ice. Lysates were centrifuged and the supernatants mixed with
122 Laemmli sample buffer containing DTT (Thermofisher). Proteins were fractionated by polyacrylamide gel
123 electrophoresis (PAGE) on 4-12% Bis-Tris polyacrylamide gels and transferred to PVDF membranes
124 (Novex). Nonspecific binding was blocked by incubation of membranes in TBST 5% BSA solution for 1
125 hour, followed by incubation with primary antibodies overnight at 4°C. Rabbit anti-ERK1/2, anti-
126 phospho-ERK(Thr202/Tyr204), anti-Pyk2, anti-phospho-Pyk2(Tyr402), and anti-Cyclophilin B antibodies
127 were purchased from Cell Signaling. HRP-conjugated anti-rabbit secondary antibody (Cell Signaling) was

128 applied to the membranes for 1 hour at room temperature. Immunoreactive products were visualized using
129 the Celvin S 420 imaging system (Biostep).

130 **Conjugation assay**

131 NK and cancer cells were differentially labeled with PKH-67 or PKH-26 membrane dyes (Sigma-Aldrich)
132 according to the manufacturer's protocol. Cells were washed 4x with serum-containing medium and
133 further kept in complete X-VIVO-10 medium at 37°C for 1 hour to wash out residual PKH and prevent
134 cross-staining. Samples were then resuspended in fresh complete X-VIVO-10 medium. 1×10^5 NK cells
135 were mixed with 2×10^5 cancer cells in a final volume of 200 μ L, centrifuged (50 x g, 1 min) and incubated
136 for 20 min at 37°C. Cell-cell interactions were stopped by brief vortexing and addition of 300 μ L of 0.5%
137 paraformaldehyde (PFA, Sigma-Aldrich). Samples were then acquired directly on a BD FACSCanto II
138 flow cytometer, and conjugates were determined as double-positive events.

139 **Confocal microscopy**

140 Conjugates between NK cells and target cells at a 1:1 ratio were formed in suspension for 5 min and
141 adhered to poly-L-lysine coated slides (Polyprep, Sigma-Aldrich) for 15 min, all at 37°C. LFA-1 was
142 blocked with anti-LFA-1 (TS1/22; Thermofisher) at a concentration of 20 μ g/mL for 1 hour at 37°C prior
143 to co-culture with target cells. Where indicated, trastuzumab (2 μ g/mL) was added. Cells were fixed and
144 permeabilized with 4% formaldehyde for 15 min at RT, permeabilized with 0.1% Triton X-100 in PBS for
145 15 min, and incubated 2x 5min in PBS containing 0.1% saponin. Slides were blocked with 1% BSA in
146 PBS containing 0.1% saponin for 30 min and labeled with antibodies specific for perforin A647 (δ G9; BD
147 Pharmingen) and β -tubulin (rabbit; Cell Signaling) for 1 hour at RT. Slides were rinsed and stained with
148 secondary anti-rabbit A555 antibody (Thermofisher) and phalloidin A488 (Life Technologies) for 1 hour
149 at RT. Slides were rinsed and covered with 0.15 mm glass coverslips (Ibidi) using Prolong Gold Antifade
150 reagent (Invitrogen) containing DAPI. Cell conjugates were visualized using a laser scanning confocal
151 microscope (LSM 880; Zeiss) by scanning through the x-y plane. Detection settings were adjusted so that
152 a control-stained sample was uniformly negative and experimental-stained samples did not saturate or
153 bleed into other channels. Images were analyzed using Fiji/ImageJ software version 1.52p (National
154 Institutes of Health) and Imaris (BitPlane). Effector and target cells in the conjugate were confirmed by
155 the presence of perforin expression. The MTOC was defined as a point with the highest density of β -
156 tubulin signal, and the immunological synapse was defined as a central point of contact of NK and target
157 cell (visualized by differential interference contrast). MTOC polarization was calculated as the shortest
158 distance from the MTOC to the immunological synapse.

159 TIRF microscopy of the immunological synapse

160 Lyophilized ErbB2-Fc protein (R&D Systems) was reconstituted with PBS following the manufacturer's
161 instructions. Purification of ICAM-1 protein, fluorophore conjugation of proteins, preparation of
162 generated supported lipid layers (SLB), microscopy setup for total internal fluorescence imaging mode,
163 measurement of antigen densities and quantitation of receptor-engaged antigens were performed as
164 previously described (7). Briefly, SLBs were loaded with ErbB2-AF555 and ICAM-1-AF488 proteins,
165 and imaging experiments were performed at antigen densities of 281.84 and 303.40 molecules/ μm^2 ,
166 respectively. In experiments imaging haNK cells in presence of trastuzumab, the imaging buffer (Hank's
167 Balanced Salt Solution containing 2 mM CaCl_2 , 2 mM MgCl_2 , 2% FBS, 10 mM HEPES) was
168 supplemented with 0.16 $\mu\text{g}/\text{mL}$ trastuzumab. Image processing was performed with the Fiji image
169 processing package (v. Madison / 7 March 2011) based on ImageJ (v. 1.5) 48,49.

170 Statistical analysis

171 Statistical analyses were performed with GraphPad Prism 7 (Graphpad Software). Unpaired two-tailed
172 Student's t-test was used for statistical calculations unless otherwise noted. A P value <0.05 was
173 considered statistically significant. **** $P < 0.0001$; *** $P < 0.001$; ** $P < 0.01$; * $P < 0.05$; ns (not significant)
174 $P \geq 0.05$.

175 SUPPLEMENTARY FIGURE LEGENDS

176

177 Figure S1: Generation of primary CAR-NK cells.

178 (A) Human primary NK cells were isolated from PBMCs of healthy donors. Isolated NK cells were
179 analyzed for purity by flow cytometry with CD3- and CD56-specific antibodies. Representative data are
180 shown. (B) Primary NK cells were transduced with a lentiviral ErbB2.CAR construct. CAR expression
181 was detected with an anti-Fab antibody 7 days after transduction. Representative data are shown.

**182 Figure S2: Effects of LFA-1 and immune checkpoint molecules on degranulation of haNK and NK-
183 92/5.28.z cells.**

184 (A) NK-92/5.28.z cells were incubated for 2 hours with plate-bound ErbB2 protein in the presence of
185 labeled anti-CD107a antibody followed by flow-cytometric analysis of CD107a. Data were pooled from 3
186 independent experiments. Mean values \pm SEM are shown. (B) haNK cells were incubated with plate-
187 bound trastuzumab and anti-LFA-1, and NK-92/5.28.z cells with ErbB2 protein, in each case combined
188 with plate-bound antibodies targeting the indicated inhibitory receptors or immune checkpoint molecules,

189 or respective isotype controls. Degranulation was measured by flow cytometric analysis of CD107a
190 expression. Red lines indicate uninhibited degranulation of controls, while blue lines represent
191 degranulation upon ligation of inhibitory receptors or immune checkpoint molecules. Representative data
192 of 3 independent experiments are shown.

193 **Figure S3: Treatment of ICAM-1 high and ICAM-1 KO cancer cells with 5AZA or TNF- α and its**
194 **effect on ADCC or CAR-mediated NK cell cytotoxicity.**

195 MDA-MB-453 cells (A, B) and MDA-MB-453 ICAM-1 KO cells (C, D) were treated with 1 μ M 5-aza-2'-
196 deoxycytidine (5AZA) for 72 hours or with 100 ng/mL TNF- α for 48 hours as indicated. (A, C) The
197 expression of ICAM-1 and ErbB2 was analyzed by flow cytometry. Representative histograms are shown.
198 (B, D) haNK cells combined with trastuzumab, haNK, or CAR-engineered NK-92/5.28.z cells were
199 incubated for 2 hours with MDA-MB-453 (B) or MDA-MB-453 ICAM-1 KO cells (D) pre-treated with
200 5AZA or TNF- α . Specific cytotoxicity was measured using a Europium-based cytotoxicity assay. Data
201 were pooled from 3 independent experiments. Mean values \pm SD are shown.

202 **Figure S4: Effect of NKG2A blockade on ADCC or CAR-mediated NK cell cytotoxicity in SKOV-3**
203 **cells.**

204 (A) Phenotypic profiling of SKOV-3 cells by flow cytometry. Representative histograms are shown. (B)
205 NK-92/5.28.z cells and haNK cells with trastuzumab were incubated with anti-NKG2A blocking antibody
206 or control IgG for 60 min followed by co-culture with SKOV-3 cells for 2 hours, and specific cytotoxicity
207 was measured using a Europium-based cytotoxicity assay. (C) Alternatively, NK cells were co-cultured
208 with SKOV-3 NuLight Red (NR) cells and cytotoxicity was measured using the IncuCyte live cell imaging
209 system for 72 hours. Data were pooled from 3 independent experiments. Mean values \pm SD are shown.

210 **Figure S5: Effect of NKG2A blockade on ADCC or CAR-mediated NK cell cytotoxicity in**
211 **HT18584-HLA-E*spG cells**

212 (A) Phenotypic profiling of HT18584-HLA-E**spG* cells by flow cytometry. Representative histograms
213 are shown. (B) NK-92/5.28.z cells and haNK cells with trastuzumab were incubated with anti-NKG2A
214 blocking antibody or control IgG for 60 min followed by co-culture with HT18584-HLA-E**spG* cells for 2
215 hours, and specific cytotoxicity was measured using a Europium-based cytotoxicity assay. Representative
216 data from three independent experiments done in triplicate are shown. Means \pm SD.

217

218 SUPPLEMENTARY REFERENCES

- 219 1. Gong JH, Maki G, Klingemann HG. Characterization of a human cell line (NK-92) with
220 phenotypical and functional characteristics of activated natural killer cells. *Leukemia*. 1994;8(4):652-8.
- 221 2. Schonfeld K, Sahm C, Zhang C, Naundorf S, Brendel C, Odendahl M, et al. Selective inhibition of
222 tumor growth by clonal NK cells expressing an ErbB2/HER2-specific chimeric antigen receptor. *Molecular*
223 *therapy : the journal of the American Society of Gene Therapy*. 2015;23(2):330-8.
- 224 3. Jochems C, Hodge JW, Fantini M, Fujii R, Morillon YM, 2nd, Greiner JW, et al. An NK cell line
225 (haNK) expressing high levels of granzyme and engineered to express the high affinity CD16 allele.
226 *Oncotarget*. 2016;7(52):86359-73.
- 227 4. Murad S, Michen S, Becker A, Fussel M, Schackert G, Tonn T, et al. NKG2C+ NK Cells for
228 Immunotherapy of Glioblastoma Multiforme. *International journal of molecular sciences*. 2022;23(10).
- 229 5. Nowakowska P, Romanski A, Miller N, Odendahl M, Bonig H, Zhang C, et al. Clinical grade
230 manufacturing of genetically modified, CAR-expressing NK-92 cells for the treatment of ErbB2-positive
231 malignancies. *Cancer immunology, immunotherapy : CII*. 2018;67(1):25-38.
- 232 6. Sanjana NE, Shalem O, Zhang F. Improved vectors and genome-wide libraries for CRISPR
233 screening. *Nature methods*. 2014;11(8):783-4.
- 234 7. Gudipati V, Rydzek J, Doel-Perez I, Goncalves VDR, Scharf L, Konigsberger S, et al. Inefficient CAR-
235 proximal signaling blunts antigen sensitivity. *Nature immunology*. 2020;21(8):848-56.

236

Fig. S1

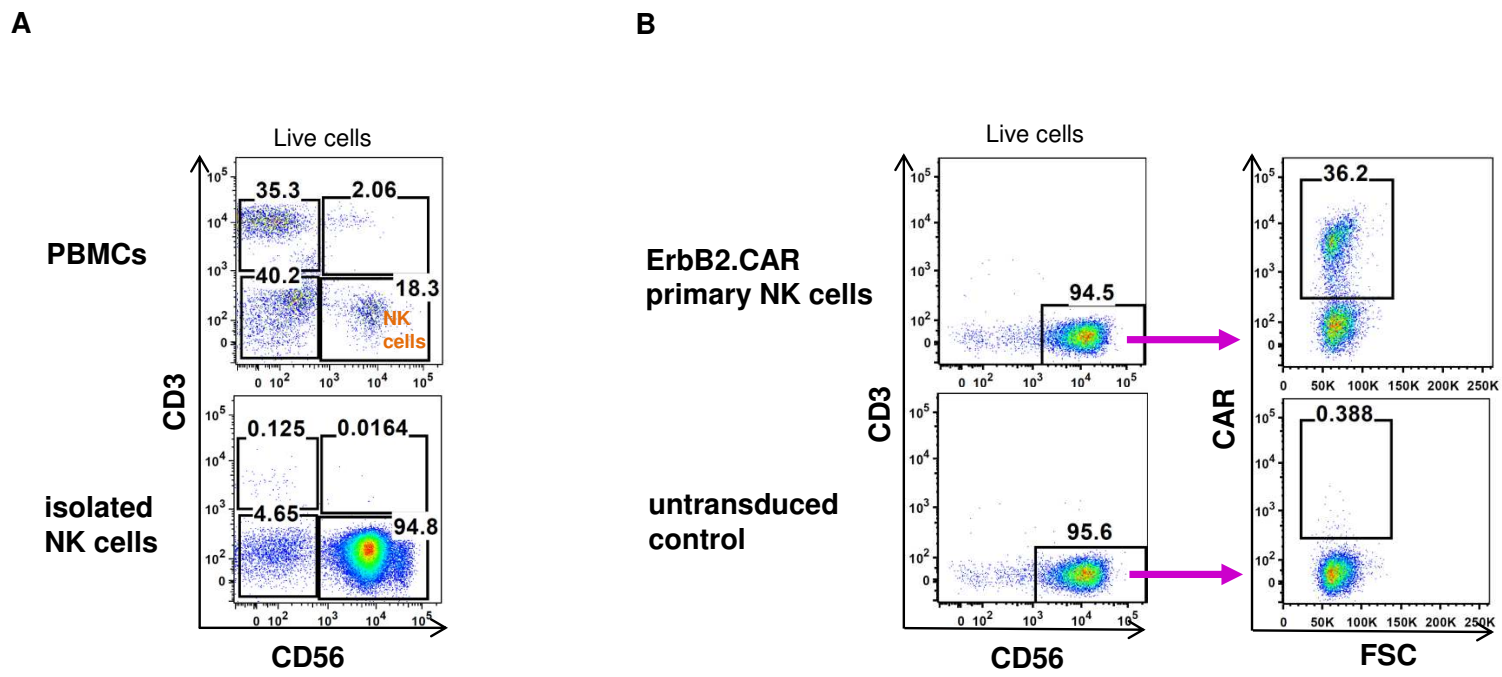


Fig. S2

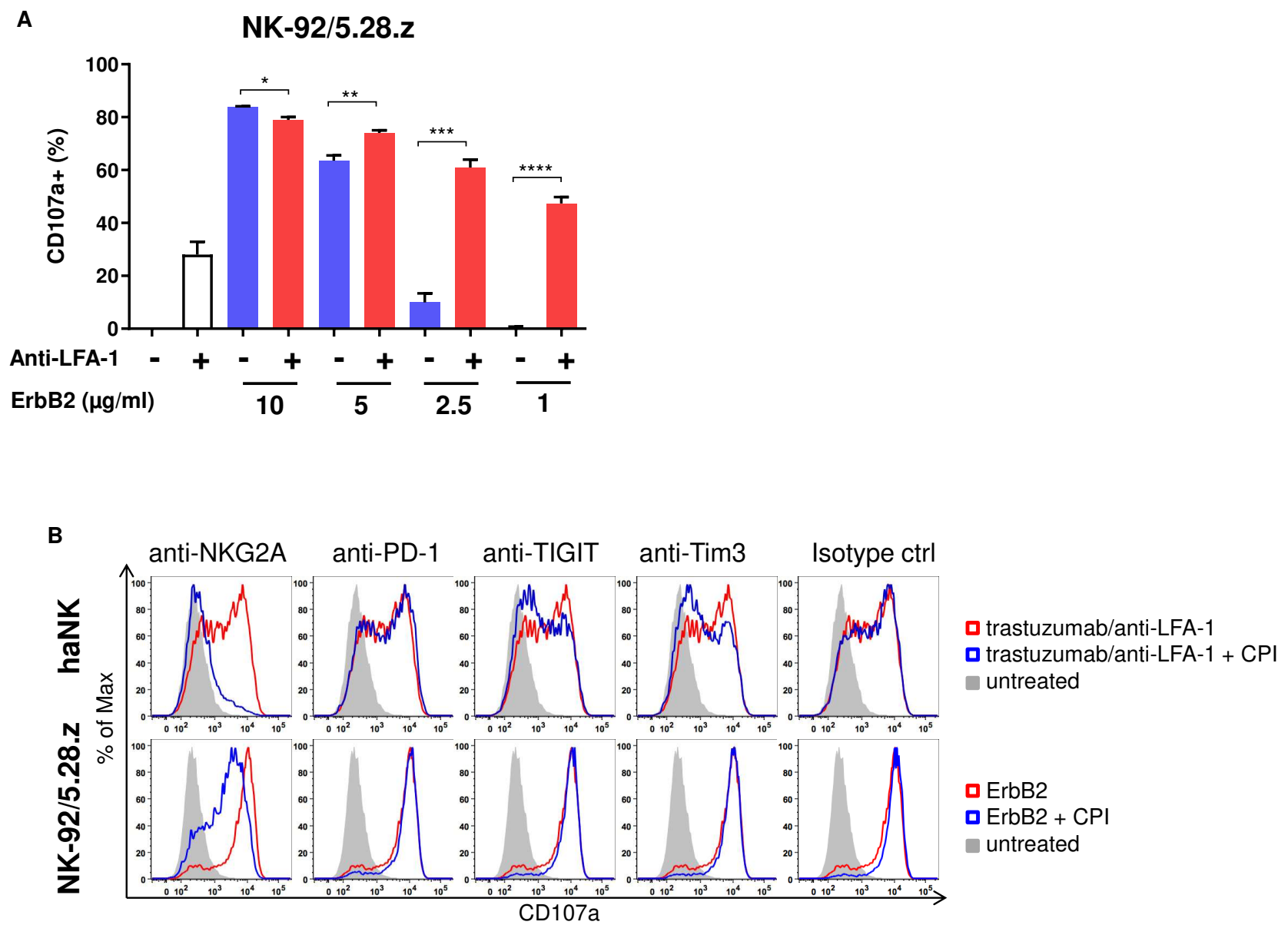


Fig. S4

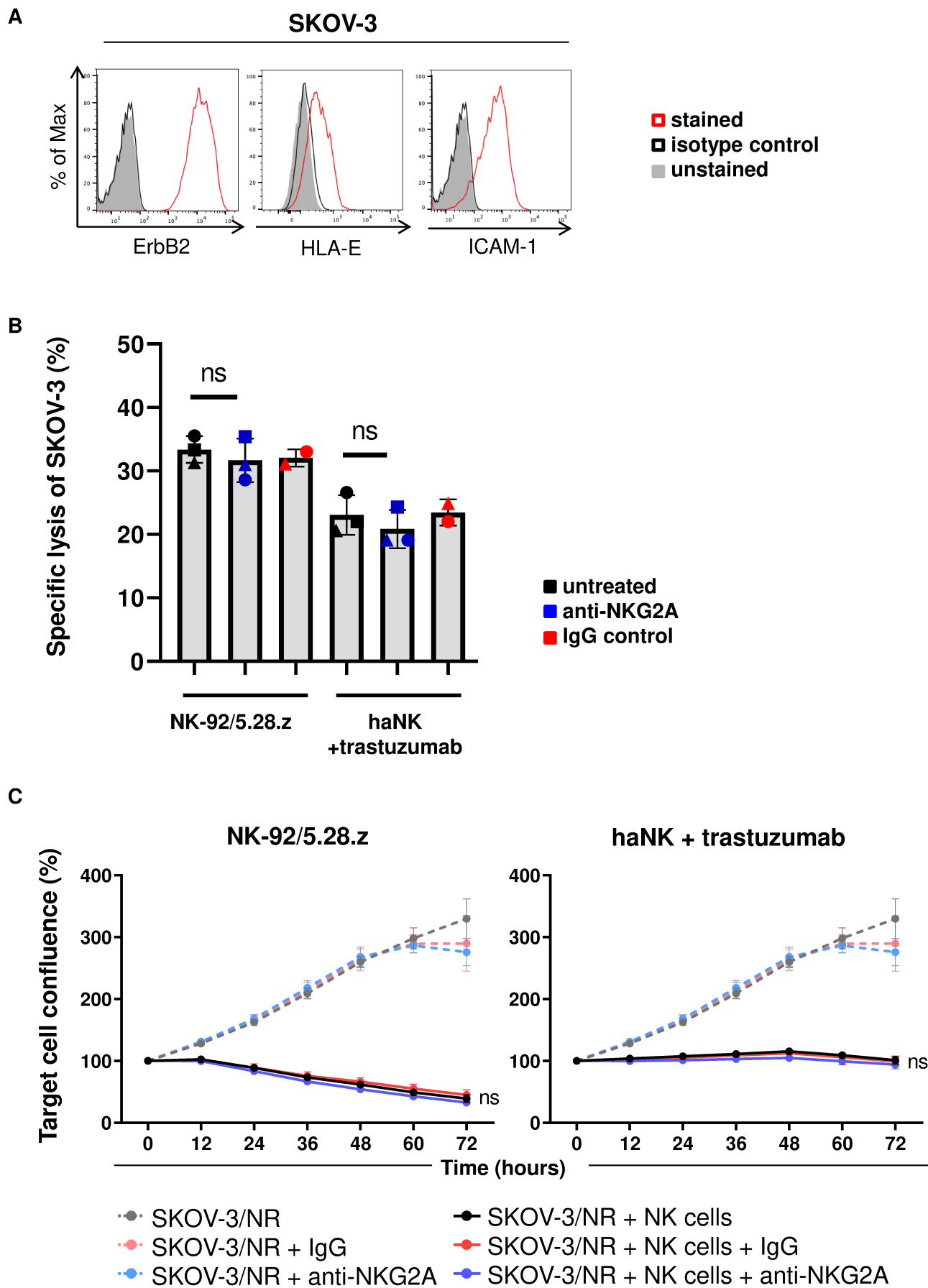


Fig. S3

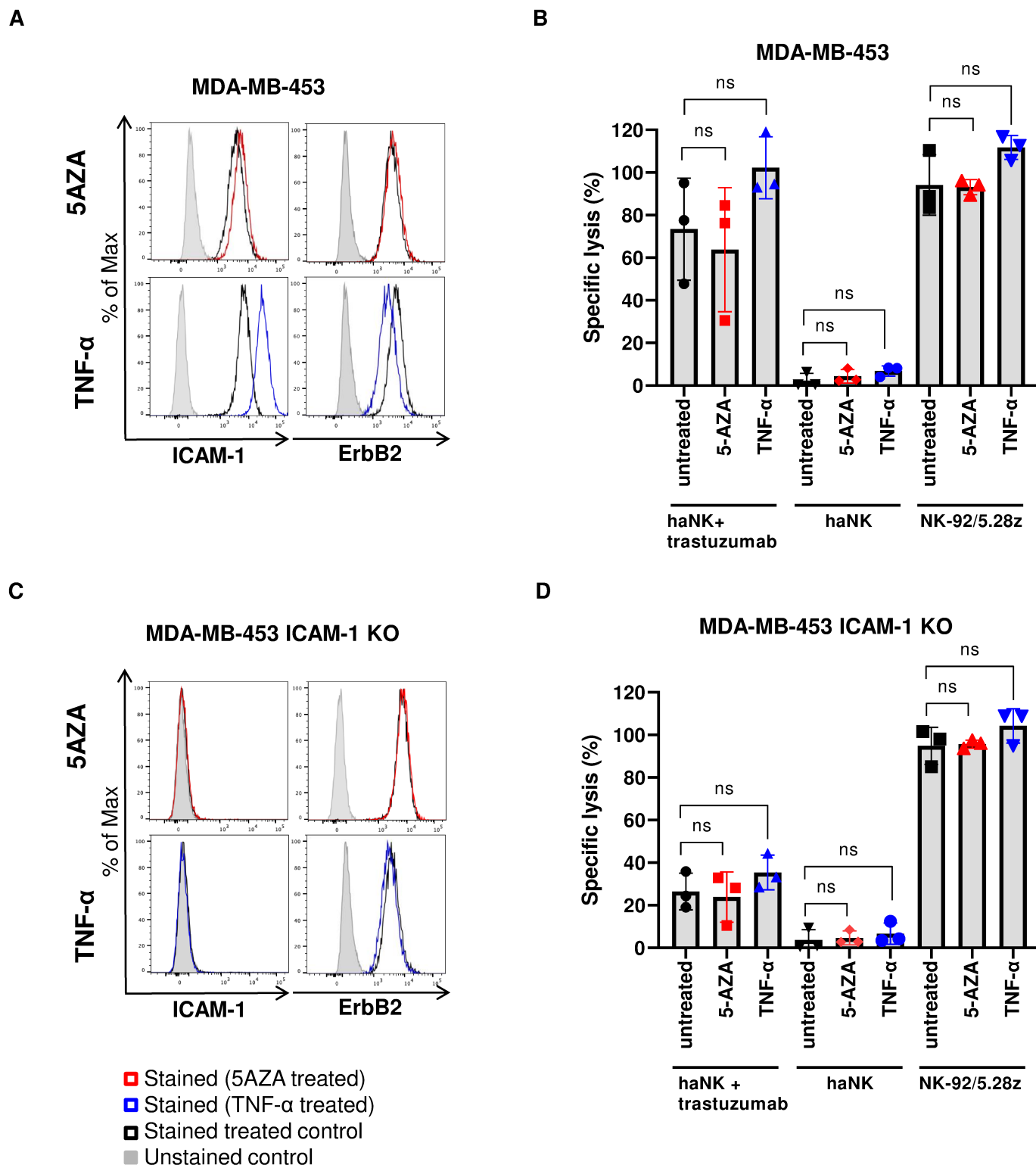


Fig. S5

